

Objective: To demonstrate a machine learning approach to optimize a new biomass-to-bioproduct conversion process, making it smart, automated, and customizable in rural communities.

Functional Requirements: If successful, our machine learning approach will be valuable to the company and our customers by delivering the following functions:

- Automatically adjust the reaction condition with minimal human intervention in light of fluctuating input biomass feedstock conditions and quality-controlled end use specifications for the output product;
- Predict and design the desired reaction set points in a completely new biomass processing scenario by drawing upon past data, and automatically update the model by incorporating new data from this new scenario;
- Predict and alert impending failures of various components to initiate a preventive repair process;
- Collect an ongoing usage fee for our software as a service model per tonne of biomass processed through our fleet of reactors deployed in the field;
- For a given bioproduct/biofuel demand/pricing condition on a given day in a given locality, optimize the production process to meet the need and deliver maximal value to the biomass suppliers and output product offtakers (i.e. an Uber model for the bioeconomy);
- For a given community input-output scenario, automatically generate a lifecycle assessment, calculate the amount of carbon avoided and/or removed, generate QR code to go on the output product packaging for verification when the carbon is indeed avoided/removed, and administer carbon payments to the relevant stakeholders in an automated fashion;
- Be generalizable for other types of bioconversion reactors/projects beyond Takachar's thermochemical process to be integrated onto our coordination platform.

Background and Significance: There is growing interest in using non-merchantable crop and forest residues, municipal food waste, and even sewage (i.e. biomass) as renewable carbon-based feedstocks for various bioproducts such as biofuels, chemicals, fertilizers, and additives [1]. This could directly replace more carbon-intensive, fossil-based feedstocks, and therefore have more than 10 gigatonnes of CO₂ equivalent per year of carbon reduction potential [2]. Yet, there are significant hurdles to the adoption of bioconversion technologies: Currently, more than 4 billion tonnes/year of biomass residues in rural communities are burned in open air instead [3]. Not only is this a significant economic waste (\$120 billion/year), but it also contributes to around 18% of all anthropogenic global warming emissions, other toxic air pollution such as particulates in urban smog, and—in Pacific North America such as British Columbia—property- and life-destroying wildfires [4].

Two major barriers exist in scaling the conversion and utilization of biomass residues. The first barrier is that raw biomass is often loose, wet, and bulky, making it logistically expensive to transport and collect in a centralized conversion facility. The second barrier is that many types of biomass are highly variable in their characteristics such as particle sizes, moisture contents, and composition. This variability poses significant challenges to the chemical conversion process. For example, certain biomass gasifiers can only run on wood chips of a narrow range of moisture

contents and particle sizes [5]. Many biodigesters likewise fail when the input feedstock composition changes significantly [6]. While the current literature is ripe with various new biomass-to-bioproduct conversion processes—both thermochemical and biological—few studies have addressed how the two above-mentioned barriers can be overcome in scaling these conversion technologies.

Our work so far was aimed at solving the first part of the bioconversion barrier (feedstock logistics). By exploring a new thermochemical process called oxygen-lean thermochemical treatment, our work led to a new class of simplified, continuous biomass thermochemical reactor designs that are small-scale, low-cost, portable, and autothermal (i.e. does not require external energy source to start or to operate) [7]. Instead of centralizing biomass from rural areas, our decentralized technology has enabled rural communities to generate and consume a wide range of bioproducts (e.g. fertilizers, biofuels, chemicals) at the source of waste generation, without having to transport the waste out of these communities. Our team demonstrated that the prototype could support stable, autothermal conversion. More importantly, we showed that this prototype allows for the precise control and adjustment of process parameters (such as air-to-biomass ratio and bioproduct removal rate) [8]. The implication of this discovery is that a wide range of input feedstock characteristics can be admitted into the reactor and transformed into quality-controlled, customizable output bioproducts, thereby simultaneously addressing the second part of the bioconversion barrier (feedstock variability).

This research proposal intends to fully explore and realize the feedstock-flexible nature of this technology by applying machine learning and optimization techniques to a growing dataset of input and output variables generated from our reactor prototypes that are actively commercialized and deployed in the field. The techniques developed in our research project could be generalized to other types of smart, decentralized, networked bioreactors deployed within self-contained communities (Figure 1). This can result in a cloud-based control system that gathers real-time biomass data and the market demand, and coordinate the reactor fleet to produce customized bioproducts meeting the specific local end user needs.

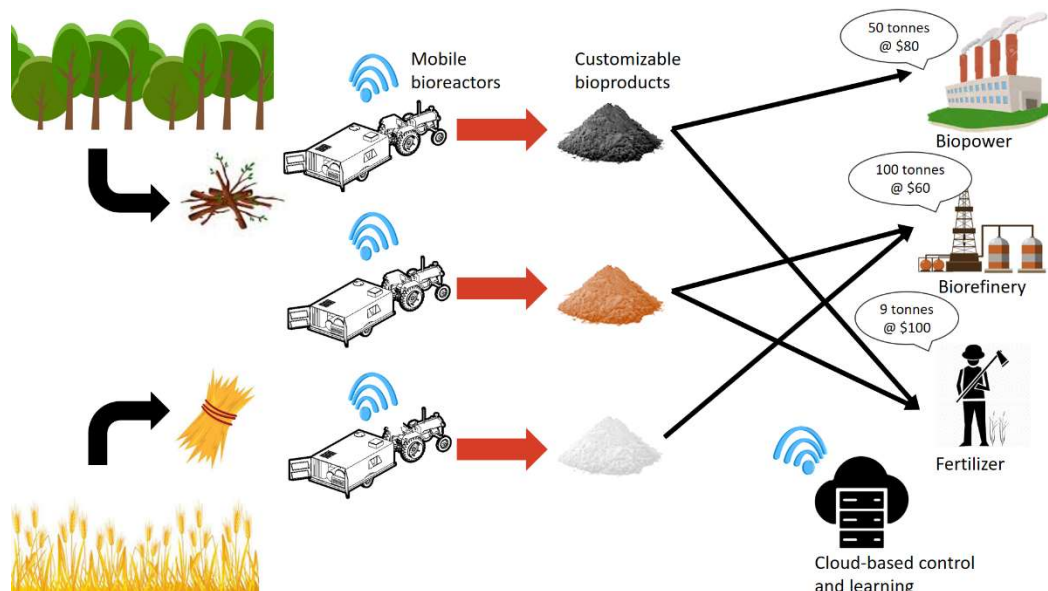


Figure 1. A vision for decentralized, on-demand, coordinated bioproduct production from local residues, driven by a smart, real-time control system that can support self-sufficient rural communities.

Research Question and Hypothesis

- What are the key features needed for the dynamic precision control of small-scale, decentralized bioconversion pathways, such as our new oxygen-lean thermochemical treatment process?
- Based on the key features above, we hypothesize that we can train a machine learning model to enable biomass reactors to learn and predict their optimal reaction configurations for new input biomass conditions and output product requirements in real time without human intervention.

Methodology: Chemical processes such as biomass thermochemical treatment are highly nonlinear, rendering traditional linear multivariate tools such as principal component analysis and partial least squares unsuitable [9]. Certain machine learning algorithms have proven to be robust in handling both non-linear and large datasets [10-13]. The approach we take is to learn from historical process data gathered from our existing prototypes actually deployed in the field, in order to update the prototype process online using a combination of transfer learning and reinforcement learning. While this project focuses on applying existing machine learning techniques to a new class of small-scale, decentralized chemical reactor processes not previously studied, new theoretical problems may emerge during our research as well.

Objective: *To instrument and collect chemical process and output data in diverse conditions*

Task 1.1: Initial process data collection – The initial continuous reactor prototype will be built and tested internally at the University of British Columbia (6301 Stadium Rd) with the input from the local Musqueam people. The prototype will be carefully instrumented with at least 10 thermocouples, 2 pressure transducers, 2 load cells (input and output sides), and gas analyzers to log high quality reactor process data needed for machine learning (Figure 2). Data will be logged with a minimum frequency of once a minute. At least three types of biomass (wood chips, and two crop residues) will be tested. For each biomass type, the prototype will be run under at least 5 different reaction configurations to produce different forms of bioproducts for subsequent laboratory characterization (details below).

Deliverable: Video of a fully realized laboratory prototype.

Measure of success: An internal prototype capable of autothermal operation under five configurations continuously for 4 hours.

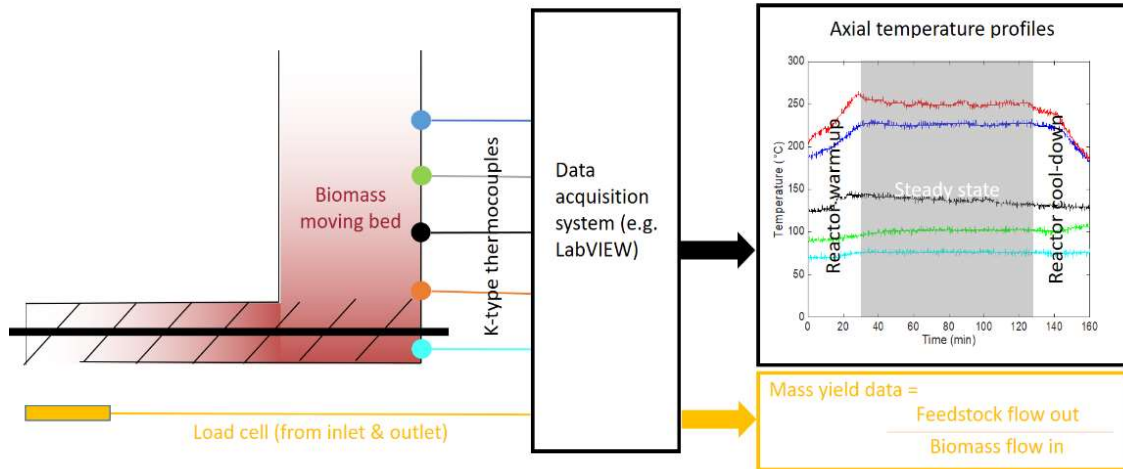


Figure 2. Instrumentation plan of the prototype to be used for collecting training data. On the right is a sample temperature-versus-time datalogging trace for a specific reactor configuration, showing an initial start-up phase, 100 min of continuous, steady-state operation, and a cool-down phase [13].

Task 1.2: Environmental data collection – Beyond the core chemical process data, various environmental data on the input (feedstock) and output (bioproduct) sides are also crucial in forming the training dataset for machine learning. Data from the incoming biomass stream will be collected on a minute-by-minute basis including moisture content (moisture meter), bulk density (load cell), and visual presentation (webcam). We will also incorporate external data, such as weather, GIS, and satellite imagery.

Deliverable: Fully annotated dataset and sources.

Measure of success: Environmental data fully synced with process data collected in Task 2.1.

Task 1.3: Output analysis – On the bioproduct output side, calorimetry (Parr 6100 Calorimeter) and ash analysis (in a muffle furnace) will be conducted at the UBC Biomass and Bioenergy Research Group (Prof. Sokhansanj). We will then dispatch the feedstock samples to various gasification plants for potential RNG production. This includes, in British Columbia, FortisBC. In California, the Pacific Gas and Electric Company has also expressed interest.

Deliverable: Dataset comprising a map of output data under different reaction conditions/configurations. Crop growth and changes in soil conditions will become part of the machine learning data.

Measure of success: Demonstrate that bioproduct characteristics can be tuned according to the reactor settings. Initial feedstock validation data (in terms of desired calorimetry value) from RNG producers.

Task 1.4: Data diversification – In order for the machine learning to be predictive in various field conditions, it is critical to collect operating data outside of the laboratory environment. Once the prototype has been adequately tested internally, we will put the prototype on a 9'

ramped trailer towered on the back of a pick-up truck to move it to different host partners' sites for a four-week-long demonstration. At each site, we will conduct the same set of internal process and environmental data collection as above. The prototype will be iterated both on-site and back at UBC to ensure better fit to end users' requirements. Different bioproducts produced under different conditions/configurations will be dispatched for laboratory analysis at UBC Biomass and Bioenergy Research Group. These results will be used to conduct a lifecycle assessment of the amount of carbon avoided and sequestered in the different production pathways in the different contexts. Initially, beyond UBC, our field test sites include: Cheakamus Community Forest, Cranbrook Community Forest, and the Regional District of Okanagan-Similkameen (see letters of support) who will serve as in-kind hosts for our project and will also provide biomass supplies to our equipment free of charge.

Deliverable: Video of field testing in at least three field sites.

Measure of success: Autothermal bioproduct generation for at least 50 hours under at least 10 reactor settings at each of the three sites.

Objective 2: Demonstrate a machine learning approach to optimize and quantify the process
In order to develop an automated control system that allows for robust customization under a range of field conditions, we need to develop the internal software capability to correlate the various inputs to desired outputs. Chemical processes such as thermochemical treatment are highly nonlinear, rendering traditional linear multivariate tools such as principal component analysis (PCA), canonical variate analysis (CVA), and partial least squares unsuitable [14]. Certain machine learning algorithms have proven to be robust in handling non-linear and large datasets [15-18]. We will learn from historical process data gathered from other existing prototypes deployed in the field, to update our new prototype online using transfer learning. The machine learning model codes and datasets will be made open-source.

Task 2.1 Extract Key Features – One challenge of applying machine learning directly to our dataset is that, the number of experiments/samples at different reactor configurations that can be feasibly performed on our biomass thermochemical treatment prototype is small (~100). To make the problem even worse, each experiment contains a large number of complex features (on the order of thousands, e.g. biomass images, a number of correlated high-resolution time-series process data), which might cause the problem of overfitting and also cloud the physical interpretability of the dominant features. One way to address this issue is feature extraction. Specifically, for the image data, we will investigate the usage of traditional image feature detection techniques, such as Features from Accelerated Segment Test (FAST) and histogram of oriented gradients (HOG). We will also explore deep learning feature extraction techniques, that is to extract hidden features from CNNs (e.g., VGG16) that have been pretrained using millions of generic images. For process data, we will explore a variety of dimensionality reduction algorithms ranging from nonlinear variants of PCA and CVA to purely nonlinear approaches such as autoencoder [19,20], local linear embedding (LLE) and ISOMAP to identify signature features of the process. Extracted features will not only be used to build machine learning models, but also serve as key real-time indicators for operators to monitor process performance.

Deliverable: List of key features and loadings.

Measure of success: Features consistently identified from different methods.

Task 2.2 Use first-principles model, other experimental datasets, and/or past prototype data for transfer learning – Another approach we will investigate to address the above-mentioned challenge is transfer learning. That is, we will pre-train the machine learning models by using *a priori* knowledge. The first source for this *a priori* knowledge is an existing multi-scale reactor model developed from first principles during our previous work [21]. This model accounts for the underlying chemical kinetics and thermodynamics of biomass thermochemical treatment [22,23], reactor-scale heat and mass transfer phenomena [24,25], as well as a reduced order technoeconomic and lifecycle assessment [26,27]. Several unknown model parameters will first be fitted using parameter estimation techniques on a small subset of new experimental data from the new local prototype. Then, the multi-scale reactor model will be used to generate millions of simulated experiments to pre-train the machine learning models. The second source for this *a priori* knowledge comprises of previous Takachar reactor data (e.g., from the California and India prototypes currently in operation under similar conditions). Once pre-trained, the model will be fine-tuned using new experimental data gathered by our field prototype, by retraining the weight of only a select few layers of the neural network model. We will evaluate the importance of different features based on the developed model via the recursive feature elimination analysis. To make our model useful to the broader community, we will make the codes open-source, which can automatically incorporate more training data, either from the same process, or from other biological or thermochemical conversion processes with different input-process-output combinations.

As an example of this approach, instead of running costly full reactor experiments under various conditions, it is possible to train a machine learning model based on thermogravimetric analysis (TGA) data, XRF data, or even spectrometer data of biomass and/or output samples. The amount of sample required for performing TGA is on the order of 10 milligrams, while that of spectrometry is on the order of a few grams, compared to hundreds of kilograms needed to run a full reactor prototype. This enables high throughput in a way that actual prototype operation may not be able to achieve. Then, the TGA and other data can be used to inform, supplement, and build a predictive machine learning model for the full reactor and its underlying chemistry. We attach in the appendix an example of such an approach using TGA.

Deliverable: Fully trained neural network model and dataset.

Measure of success: Neural model is able to converge based on the key features identified in Task 2.1.

Task 2.3 Model validation – The dataset gathered in Objectives 1-2 will train our model. The goal of this Task is to test the effectiveness of the model to update the process in real-time in the following new scenarios: (1) Processing a new type of biomass feedstock at our field prototype and testing whether the algorithm can identify and map stable operating conditions; and (2) processing an existing type of biomass feedstock under field-like, unpredictable, and fluctuating conditions.

Deliverable: Bioproduct characteristic data from the validation experiments.

Measure of success: The algorithm can maintain quality control of the output product at a specified fixed carbon value within a $\pm 5\%$ error range.

Task 2.4 Usage fee sandbox – Based on the operational data above, we will sandbox a pilot where we charge end users an ongoing usage fee based on the amount of biomass processed (e.g. tipping fee avoidance).

Deliverable: Outcome of a sandbox experiment with one user.

Measure of success: Per-tonne usage fee successfully processed and received.

APPENDIX: AN EXAMPLE OF USING THERMOGRAVIMETRIC DATA PREDICTIVELY

Introduction:

Various types of reactor designs are known to have spatial inhomogeneities in temperature and reaction conditions due to heat loss from the reactor bed to the liner and surrounding environment. This heat loss to the liner when combined with the response delay of thermocouples means that a lower temperature rise is measured than the theoretical or desired maximum temperature (Kooiman). It is important to quantify these inhomogeneities as they can have a material effect on the quality control of the output products, whether as solid charcoal, liquid bio-oil, or syngas.

Accurate measurements of precise temperature history of individual biomass particles within a reactor are difficult without the use of a number of thermocouples strategically placed throughout the reactor [cite]; however, the use of thermocouples can lead to other issues. For example, an extensive network of dozens of thermocouples is needed for a thorough enough understanding of the temperature distribution within the reactor to determine the radial temperature gradient, which provides a potentially significant material constraint (Spallina). Thermocouples can also be invasive enough to disrupt the natural reaction process when used in large quantities, which are often necessary for sufficiently useful measurements (Touitou). This is especially true if the laboratory-scale reactor under consideration is small ([Kung et al., 2018](#)).

In lieu of directly measuring a given reactor's temperature profile in detail, another potentially viable approach is to examine the distribution of key features of the output product as a proxy for the degree of inhomogeneity inside the reaction chamber. In the case of biomass torrefaction, for example, we could randomly sample torrefied biomass particles from the output stream and understand how they vary from one another in key thermal and chemical parameters as an indication of the spread in the severity of the reaction treatment within the reaction chamber.

In the past, key thermal parameters of TG/DTG analysis have been used to predict key features of biomass particles. TGA/DTG analysis has been shown to accurately describe the pyrolysis kinetics of coconut biomass particles (Rajendra), the char and fixed carbon yields from various wood biomass particles (Wang), and the co-pyrolysis behavior of brown coal and wheat straw biomass particles (Zhou).

Our hypothesis is that we can use key thermal parameters from TG/DTG analysis to predict the distribution of maximum temperature—and hence the reaction severity—experienced by individual randomly selected pine shaving biomass particles inside the reaction zone, by applying various machine learning models. This will then allow us to use literature performance metrics to identify the most effective model for temperature history prediction.

3. Results and Discussion

3.1. Simulated Biomass Properties

To collect training data for maximum temperature predictive models, we first needed to simulate the conditions of the moving bed torrefaction reactor in a measurable way. As previously stated, biomass samples were heated in an electric furnace in an inert environment from 25°C to temperatures ranging from 230°C to 450°C, at heating rates varying from 5 to 30 °C/min. Maximum temperature and heating rate were identified as key components of biomass production in literature (Yavari,Somerville), and were thus deemed relevant and feasible to predict. Fig.1 shows the various simulated maximum temperature and heating rate conditions as measured within the electric furnace.

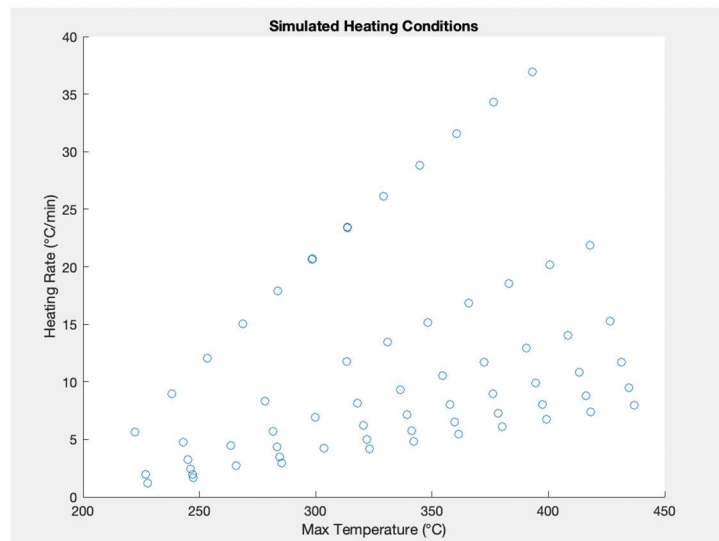


Figure 1

The various simulated maximum temperatures from 230°C to 450°C and heating rates from 5 to 30 °C/min, as precisely measured within the electric furnace. Each point represents one biomass particle.

Proximate Analysis was used to determine Volatile matter, Ash, and Fixed Carbon content of the simulated biomass samples, both in terms of proportion of total mass and absolute mass. Moisture content was neglected as all moisture content would have already been removed through the process of simulating the production of the biomass particles directly before proximate analysis. The volatile

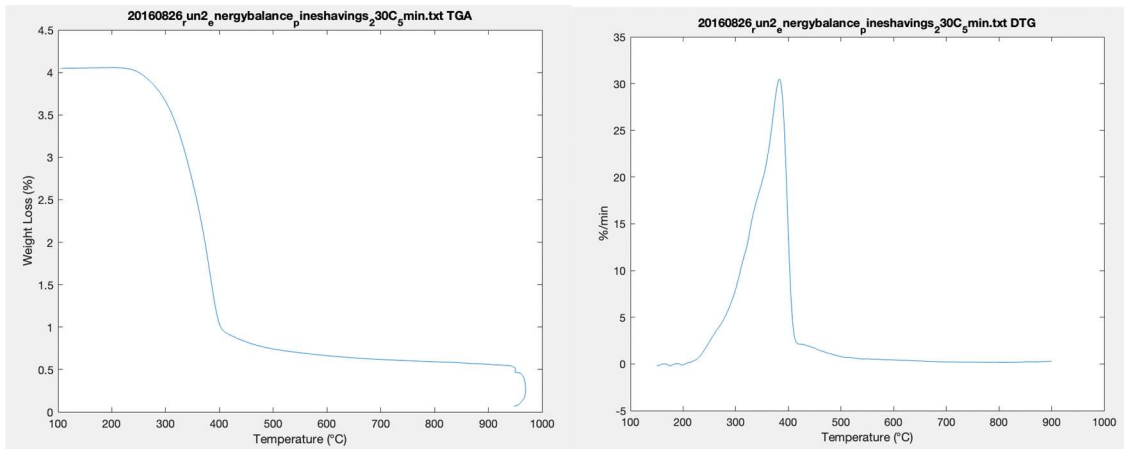
matter, ash, and fixed carbon content of the samples ranged from 36-60%, 2-9 wt. %, and 8-60% respectively.

The results of proximate analysis are reported in Table 1, along with thermochemical characteristics of the samples determined through thermogravimetric and derivative thermogravimetric analysis. The reported thermochemical characteristics include the maximum rate of weight loss (R_{\max}), temperature where maximum rate of weight loss occurs (T_{\max}), (Iordanidis),(Vasileiadou) and fixed carbon proportion on a dry-ash free basis (FC)(Ronsse) .

The values included on the TG plots are directly measured within the TA Q50 thermogravimetric analyzer.

Várhegyi and Till identify spline smoothing as a method to smooth and differentiate TG data (Várhegyi)(Chen). DTG values were calculated by first using spline smoothing with a smoothing parameter of 0.98 on the TG values to eliminate noise and the extraneous spikes it can cause, before differentiating the resulting function and inverting the values to obtain the DTG plot values. Fig. 2 shows the TG/DTG plots for the simulated biomass particles prepared in both the lowest and highest ramp temperature: 222.4°C and 436.9°C respectively (filenames: 20160826_run2_energybalance_pineshavings_230C_5min.txt and 20160928_run4_energybalance_pineshavings_450C_30min.txt). The TG/DTG plots for all 67 simulated biomass samples can be found in Appendix A.

a.



b.

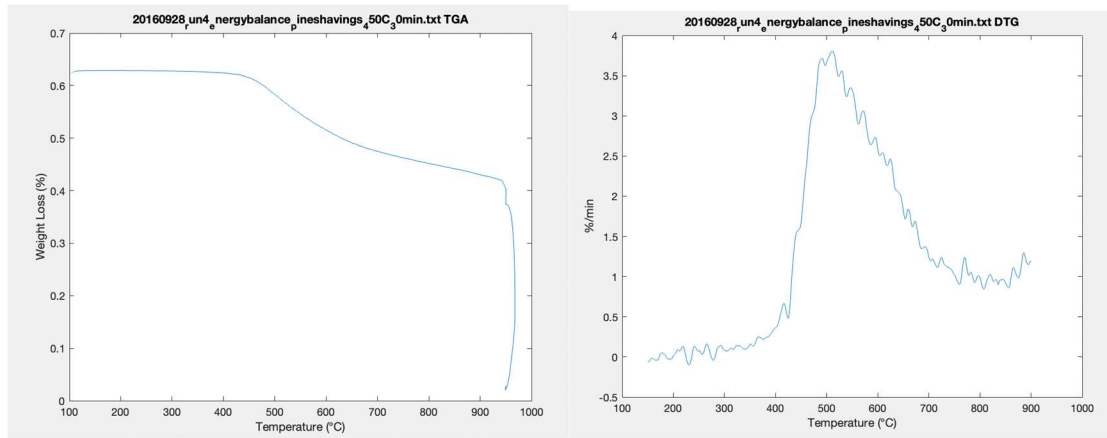


Figure 2. TG/DTG (left/right) graphs of the biomass samples labeled a. 20160826_run2_energybalance_pineshavings_230C_5min.txt and b. 20160928_run4_energybalance_pineshavings_450C_30min.txt.

Maximum rate of weight loss (R_{\max}) is calculated as the height of the peak of the DTG curve and T_{\max} is temperature the DTG peak occurs at. FC proportion (FC) is calculated by dividing the mass of fixed carbon for a biomass sample by the combined mass of fixed carbon and volatile matter of the sample.

filenames	ramptemp	rate	Rmax	Tmax	FC	Vmasspr	FCmassprop	Ashmassprop	initialmass	Vmass	Cmass	Ashmass
20160826_run2_energybalance_pineshavings_230C_5min.txt	222.4	5.61	30.49	382.91	0.1188	0.8651	0.1166	0.0183	4.046	3.5	0.472	0.074
20160826_run3_energybalance_pineshavings_270C_5min.txt	253.5	12.07	31.8	383.08	0.1301	0.8524	0.1274	0.0201	6.374	5.433	0.812	0.128
20160826_run4_energybalance_pineshavings_230C_25min.txt	227.8	1.18	31.09	382.94	0.1128	0.8744	0.1111	0.0145	5.376	4.7	0.597	0.078
20160827_run1_energybalance_pineshavings_310C_5min.txt	283.7	17.91	34.29	382.88	0.1294	0.8512	0.1265	0.0223	3.883	3.305	0.491	0.087
20160827_run3_energybalance_pineshavings_310C_15min.txt	299.9	6.92	36.2	381.88	0.1481	0.8385	0.1457	0.0158	3.556	2.982	0.518	0.056
20160830_run1_energybalance_pineshavings_230C_15min.txt	227.1	1.96	30.72	382.92	0.0828	0.9034	0.0815	0.0151	5.351	4.834	0.436	0.081
20160831_run1_energybalance_pineshavings_270C_15min.txt	263.5	4.48	32.16	382.63	0.1231	0.8562	0.1202	0.0236	7.036	6.024	0.845	0.166
20160831_run2_energybalance_pineshavings_270C_25min.txt	265.8	2.73	32.56	382.22	0.1126	0.8632	0.1096	0.0272	5.068	4.374	0.555	0.138
20160901_run1_energybalance_pineshavings_310C_25min.txt	303.5	4.26	36.5	381.89	0.156	0.8216	0.1519	0.0265	6.23	5.119	0.946	0.165
20160907_run1_energybalance_pineshavings_250C_30min.txt	247.5	1.65	30.13	380.44	0.1089	0.8491	0.1037	0.0472	5.08	4.313	0.527	0.24
20160907_run2_energybalance_pineshavings_250C_5min.txt	238.1	8.98	30.22	382.65	0.124	0.8513	0.1205	0.0283	5.887	5.011	0.709	0.167
20160907_run3_energybalance_pineshavings_290C_5min.txt	268.7	15.01	32.04	382.88	0.1339	0.8434	0.1304	0.0263	6.263	5.282	0.817	0.164
20160907_run4_energybalance_pineshavings_290C_30min.txt	285.4	2.93	34.7	381.98	0.1358	0.8342	0.1311	0.0347	2.802	2.338	0.367	0.097
20160908_run1_energybalance_pineshavings_250C_20min.txt	246.3	2.44	31.38	382.95	0.1229	0.8551	0.1198	0.0251	4.541	3.884	0.544	0.114
20160908_run2_energybalance_pineshavings_290C_20min.txt	283.3	4.33	34.64	382.66	0.1322	0.8444	0.1286	0.027	3.088	2.607	0.397	0.083
20160908_run3_energybalance_pineshavings_250C_10min.txt	243.1	4.75	30.44	382.42	0.1295	0.8468	0.126	0.0272	5.385	4.56	0.679	0.146
20160908_run4_energybalance_pineshavings_290C_10min.txt	278.3	8.32	31.95	380.94	0.1403	0.8278	0.135	0.0372	4.697	3.889	0.634	0.175
20160909_run1_energybalance_pineshavings_250C_25min.txt	247	1.96	31.01	382.61	0.1297	0.8461	0.1261	0.0278	5.527	4.677	0.697	0.154
20160909_run2_energybalance_pineshavings_290C_15min.txt	281.5	5.7	32.5	381.17	0.1382	0.8242	0.1322	0.0436	3.367	2.775	0.445	0.147
20160909_run3_energybalance_pineshavings_250C_15min.txt	245.2	3.23	30.59	382.13	0.1239	0.8551	0.121	0.0239	3.595	3.074	0.435	0.086
20160909_run4_energybalance_pineshavings_290C_25min.txt	284.6	3.5	35.53	386.27	0.1245	0.8642	0.1229	0.0129	4.832	4.176	0.594	0.062
20160914_run1_energybalance_pineshavings_330C_5min.txt	298.6	20.7	35.96	386.57	0.1115	0.8662	0.1087	0.025	2.064	1.788	0.224	0.052
20160914_run2_energybalance_pineshavings_330C_10min.txt	313.3	11.76	38.52	385.8	0.1511	0.8361	0.1488	0.0151	3.349	2.8	0.498	0.05
20160914_run3_energybalance_pineshavings_330C_15min.txt	318	8.14	39.55	385.58	0.1481	0.8262	0.1437	0.0301	2.676	2.211	0.384	0.081
20160925_run3_energybalance_pineshavings_330C_20min.txt	320.6	6.2	37.4	388.15	0.1776	0.8208	0.1773	0.0019	3.56	2.922	0.631	0.007
20160926_run2_energybalance_pineshavings_330C_25min.txt	322	5.01	38.27	387.73	0.1782	0.8163	0.1771	0.0067	3.013	2.459	0.533	0.02
20160926_run3_energybalance_pineshavings_330C_30min.txt	323.2	4.2	39.06	387.52	0.1772	0.8147	0.1754	0.0099	2.626	2.139	0.461	0.026
20160926_run5_energybalance_pineshavings_350C_30min.txt	342.1	4.83	35.76	384.77	0.2284	0.7555	0.2236	0.0209	1.973	1.491	0.441	0.041
20160927_run1_energybalance_pineshavings_350C_5min.txt	313.6	23.38	37.35	388.9	0.1462	0.8392	0.1437	0.0171	3.31	2.778	0.476	0.057
20160927_run2_energybalance_pineshavings_350C_10min.txt	330.8	13.47	39.83	387.64	0.1759	0.8099	0.1728	0.0173	3.259	2.639	0.563	0.056
20160927_run3_energybalance_pineshavings_330C_5min.txt	298.3	20.65	34.85	389.57	0.1341	0.8539	0.1322	0.0139	4.117	3.515	0.544	0.057
20160927_run4_energybalance_pineshavings_330C_10min.txt	313.2	11.74	37.85	388.38	0.1465	0.8422	0.1446	0.0133	3.463	2.917	0.501	0.046
20160928_run1_energybalance_pineshavings_350C_5min.txt	313.6	23.45	38.07	388.88	0.1358	0.8457	0.1329	0.0214	2.246	1.899	0.298	0.048
20160928_run2_energybalance_pineshavings_350C_15min.txt	336.2	9.34	40.02	386.89	0.1923	0.7906	0.1882	0.0212	2.575	2.036	0.485	0.055
20160928_run3_energybalance_pineshavings_350C_20min.txt	339.2	7.13	38.44	386.23	0.2089	0.777	0.2052	0.0178	3.106	2.414	0.637	0.055
20160928_run4_energybalance_pineshavings_450C_30min.txt	436.9	7.99	3.8	510.78	0.6245	0.3582	0.5959	0.0459	0.625	0.224	0.373	0.029
20160929_run1_energybalance_pineshavings_430C_30min.txt	418.2	7.38	5.02	475.81	0.5648	0.4117	0.5344	0.0539	1.068	0.44	0.571	0.058
20160929_run2_energybalance_pineshavings_430C_25min.txt	416.1	8.77	5.2	471.07	0.53	0.4393	0.4954	0.0653	0.744	0.327	0.369	0.049
20160929_run3_energybalance_pineshavings_430C_20min.txt	413.2	10.82	5.77	463.69	0.5283	0.4418	0.4948	0.0634	0.791	0.35	0.392	0.05
20160929_run4_energybalance_pineshavings_410C_30min.txt	399.2	6.74	6.76	455.61	0.4898	0.4778	0.4587	0.0635	0.687	0.328	0.315	0.044
20160930_run1_energybalance_pineshavings_370C_5min.txt	329.2	26.11	39.6	388.09	0.1546	0.8325	0.1522	0.0153	3.672	3.057	0.559	0.056
20160930_run3_energybalance_pineshavings_430C_15min.txt	408.5	14.06	6.42	456.55	0.5482	0.4305	0.5224	0.0471	1.039	0.447	0.543	0.049
20160930_run4_energybalance_pineshavings_430C_10min.txt	400.6	20.18	7.03	453.43	0.5273	0.4501	0.502	0.0479	1.009	0.454	0.506	0.048
20161001_run1_energybalance_pineshavings_390C_5min.txt	344.8	28.83	39.87	387.12	0.1818	0.7991	0.1776	0.0233	2.551	2.039	0.453	0.059
20161001_run2_energybalance_pineshavings_450C_5min.txt	393.2	36.96	7.52	442.47	0.4784	0.4885	0.448	0.0635	0.679	0.332	0.304	0.043
20161001_run3_energybalance_pineshavings_390C_30min.txt	380.1	6.1	8	441.3	0.477	0.4951	0.4516	0.0533	0.877	0.434	0.396	0.047
20161001_run4_energybalance_pineshavings_370C_30min.txt	361.4	5.48	18.6	378.35	0.3167	0.6518	0.3022	0.046	0.974	0.635	0.294	0.045
20161002_run1_energybalance_pineshavings_350C_25min.txt	341.2	5.77	37.56	384.92	0.1918	0.7897	0.1874	0.023	2.042	1.613	0.383	0.047
20161003_run1_energybalance_pineshavings_410C_5min.txt	360.7	31.57	32.77	383.46	0.2447	0.7389	0.2395	0.0216	2.499	1.847	0.599	0.054
20161003_run2_energybalance_pineshavings_410C_25min.txt	397.4	8.02	7.02	451.54	0.517	0.4589	0.4912	0.0499	1.001	0.459	0.492	0.05
20161005_run1_energybalance_pineshavings_430C_5min.txt	376.5	34.33	15.04	377.59	0.3794	0.5952	0.3639	0.0409	1.554	0.925	0.565	0.064

20161005_run2_energybalance_pineshavings_450C_25min.txt	434.7	9.51	4	496.1	0.5872	0.3839	0.546	0.0701	0.745	0.286	0.407	0.052
20161011_run1_energybalance_pineshavings_370C_10min.txt	348.3	15.16	37.69	385.9	0.1956	0.7877	0.1916	0.0207	2.139	1.685	0.41	0.044
20161011_run2_energybalance_pineshavings_370C_25min.txt	359.8	6.52	23.97	380.03	0.2913	0.6743	0.2772	0.0486	1.055	0.711	0.292	0.051
20161012_run1_energybalance_pineshavings_450C_10min.txt	417.8	21.87	5.64	462.19	0.5652	0.4036	0.5248	0.0716	0.841	0.34	0.442	0.06
20161012_run2_energybalance_pineshavings_450C_20min.txt	431.5	11.73	4.29	483.1	0.5987	0.3651	0.5448	0.0901	0.871	0.318	0.474	0.078
20161012_run3_energybalance_pineshavings_450C_20min_rep	431.4	11.72	4.19	486.69	0.5705	0.4222	0.5608	0.017	0.643	0.272	0.361	0.011
20161012_run4_energybalance_pineshavings_370C_15min.txt	354.4	10.53	33.64	383.74	0.2049	0.7625	0.1965	0.041	0.987	0.752	0.194	0.04
20161013_run1_energybalance_pineshavings_410C_10min.txt	383.1	18.53	7.67	441.05	0.4727	0.5042	0.452	0.0438	1.232	0.621	0.557	0.054
20161013_run2_energybalance_pineshavings_410C_15min.txt	390.6	12.92	7.52	447.05	0.5173	0.463	0.4962	0.0408	1.338	0.619	0.664	0.055
20161013_run3_energybalance_pineshavings_410C_20min.txt	394.7	9.89	7.22	449.68	0.5452	0.4368	0.5236	0.0396	1.707	0.746	0.894	0.068
20161014_run1_energybalance_pineshavings_390C_10min.txt	365.6	16.83	25.14	380.81	0.3175	0.665	0.3094	0.0256	2.721	1.81	0.842	0.07
20161014_run2_energybalance_pineshavings_390C_15min.txt	372.3	11.71	12.57	377.17	0.4134	0.5677	0.4	0.0323	2.118	1.203	0.847	0.068
20161014_run3_energybalance_pineshavings_390C_20min.txt	376	8.97	7.74	436.08	0.4905	0.4914	0.4731	0.0355	2.165	1.064	1.024	0.077
20161014_run4_energybalance_pineshavings_390C_25min.txt	378.4	7.26	7.91	439.69	0.5014	0.4845	0.4873	0.0282	1.43	0.693	0.697	0.04
20161015_run1_energybalance_pineshavings_450C_15min.txt	426.6	15.29	4.73	474.38	0.5542	0.4142	0.5149	0.0709	0.568	0.235	0.292	0.04
20161015_run2_energybalance_pineshavings_370C_20min.txt	357.7	8.06	28.56	381.76	0.2676	0.7109	0.2597	0.0294	1.508	1.072	0.392	0.044

Table 1 contains the results of proximate and TG/DTG analysis, along with the corresponding simulation ramp temperature and heating rate.

With key thermal parameters identified for each biomass particle through TG/DTG analysis, we follow the strategy utilized in Cleveland of analyzing data through a scatterplot matrix to determine dependence of response variables on predictive variables in order to potentially predict maximum temperature and heating rate in our case. Fig. 3 is a scatterplot matrix of response variable (maximum temperature, heating rate) against predictive thermal parameters (Tmax, Rmax, FC).

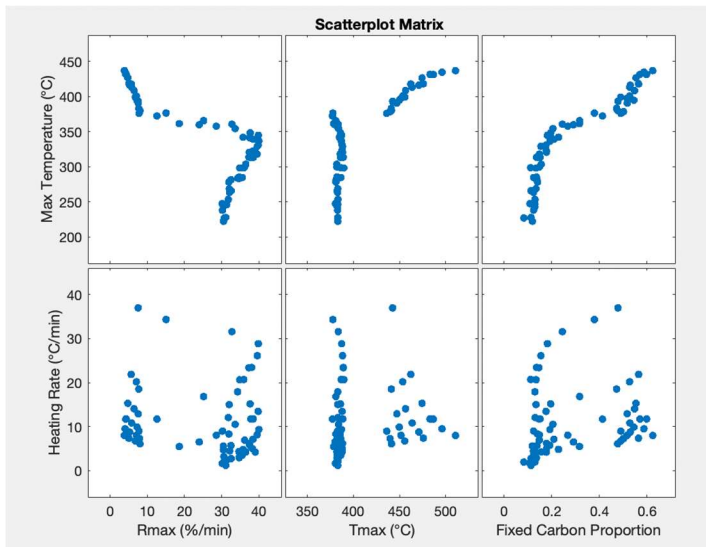


Figure 3

The figure is a scatterplot matrix of 67 measurements of maximum temperature and heating rate experienced by biomass samples, and the resultant thermal parameters Rmax, Tmax, and fixed carbon proportion determined through TG/DTG analysis. The goal being to predict maximum temperature and heating rate from the thermal parameters.

As is evident in the scatterplot matrix, there is a much stronger relationship between maximum temperature and the thermal parameters than between heating rate and the thermal parameters. This implies that the maximum temperature predictions will likely be more accurate than heating rate predictions, and thus we will use machine learning models to predict the maximum temperature experienced by biomass particles, with heating rate being an important consideration of potential noise in the maximum temperature data; properly considering noise in data is essential to creating a more robust model, from image resolution enhancement (Farsiu) to neural network-based speech recognition (Tóth). Thus, heating rate acts as noise, which when included ultimately strengthens our maximum temperature predictions, as heating rate can still be a key component to biomass production even if not predictable using our thermal components.

There is also a discontinuity evident between 350-390 °C on the three graphs plotting maximum temperature against the thermal parameters. Cellulose found in biomass samples, including pine, has been shown to break down at this temperature range (Yang)(Anca-Couce)(Akhtar), likely leading to changes in the characteristic composition of the biomass particles during preparation and thus altering their measured thermal parameters.

3.2. Performances of Machine Trained Models

The results of all selected machine trained models for predicting maximum biomass preparation temperature are provided in Table 2. The average and standard deviation of RMSE, RRMSE, MBE, MPE, and R^2 (Bouchouicha, et.al) across 100 repetitions (Nakatsu, et.al) of 10-fold cross validation are reported.

Model	RMSE (°)	RRMSE(%)	MBE(°)	MPE(%)	R^2
M1	13.584	4.067	-0.011	0.207	0.95
(SD)	0.187	0.056	0.152	0.046	0.001
M2	13.121	3.928	-0.329	0.092	0.953
(SD)	0.355	0.106	0.206	0.059	0.003

M3	13.598	4.071	0.039	0.225	0.95
(SD)	0.209	0.062	0.128	0.039	0.002
M4	13.655	4.088	-0.027	0.202	0.949
(SD)	0.336	0.101	0.178	0.051	0.003
M5	10.274	3.076	0.001	0.137	0.971
(SD)	0.554	0.166	0.701	0.208	0.003
M6	18.021	5.395	-0.59	0.161	0.912
(SD)	0.578	0.173	0.742	0.233	0.006
M7	61.61	18.445	-0.013	3.63	-0.031
(SD)	0.375	0.112	0.063	0.027	0.013
M8	13.852	4.147	-0.323	0.093	0.948
(SD)	0.319	0.095	0.306	0.106	0.002
M9	12.684	3.797	-0.502	-0.115	0.956
(SD)	0.947	0.283	0.506	0.147	0.007
M10	12.614	3.776	-0.722	-0.133	0.954
(SD)	3.45	1.033	1.202	0.342	0.039
M11	12.004	3.594	-1.175	-0.011	0.961

(SD)	0.831	0.249	0.339	0.091	0.006
M12	10.874	3.256	-0.423	0.196	0.968
(SD)	0.419	0.126	0.311	0.107	0.002
M13	29.875	8.944	5.251	3.039	0.758
(SD)	0.306	0.092	0.232	0.077	0.005
M14	17.509	5.242	-14.63	-4.257	0.917
(SD)	0.462	0.138	0.46	0.148	0.004
M15	14.168	4.242	-1.37	0.072	0.945
(SD)	0.801	0.24	0.56	0.182	0.006
M16	8.53	2.554	-0.148	0.039	0.98
(SD)	0.474	0.142	0.305	0.09	0.002
M17	8.592	2.572	-0.421	-0.041	0.98
(SD)	0.539	0.161	0.369	0.118	0.003
M18	7.403	2.216	-0.439	-0.059	0.985
(SD)	0.285	0.085	0.205	0.066	0.001
M19	8.583	2.57	-0.439	-0.039	0.98
(SD)	0.364	0.109	0.38	0.125	0.002

M20	11.282	3.378	0.657	0.236	0.964
(SD)	1.978	0.592	0.944	0.274	0.015
M21	11.472	3.435	0.399	0.131	0.963
(SD)	2.064	0.618	1.16	0.351	0.015
M22	11.462	3.431	-0.058	-0.083	0.963
(SD)	2.203	0.659	1.064	0.321	0.016
M23	11.611	3.476	0.555	0.219	0.962
(SD)	2.245	0.672	0.844	0.261	0.018
M24	12.015	3.597	0.339	0.167	0.958
(SD)	2.937	0.879	1.249	0.412	0.024

Table 2 contains the average and standard deviation of RMSE, RRMSE, MBE, MPE, and R^2 across 100 repetitions of 10-fold cross validation for the selected machine trained models.

The results of all 24 selected machine trained models for predicting maximum biomass preparation temperature are provided in Table 2. The average and standard deviation of RMSE, RRMSE, MBE, MPE, and R^2 (Bouchouicha, et.al) across 100 repetitions (Nakatsu, et.al) of 10-fold cross validation are reported.

Fig. 4.a-d compares the 95% confidence intervals of the RMSE, MBE, MPE, and R^2 respectively for each model, excluding M6,M7,M13, and M14. These models had poor performance metrics, specifically RMSE and R^2 , demonstrating their weak predictive capabilities and were removed for improved readability of the confidence intervals.

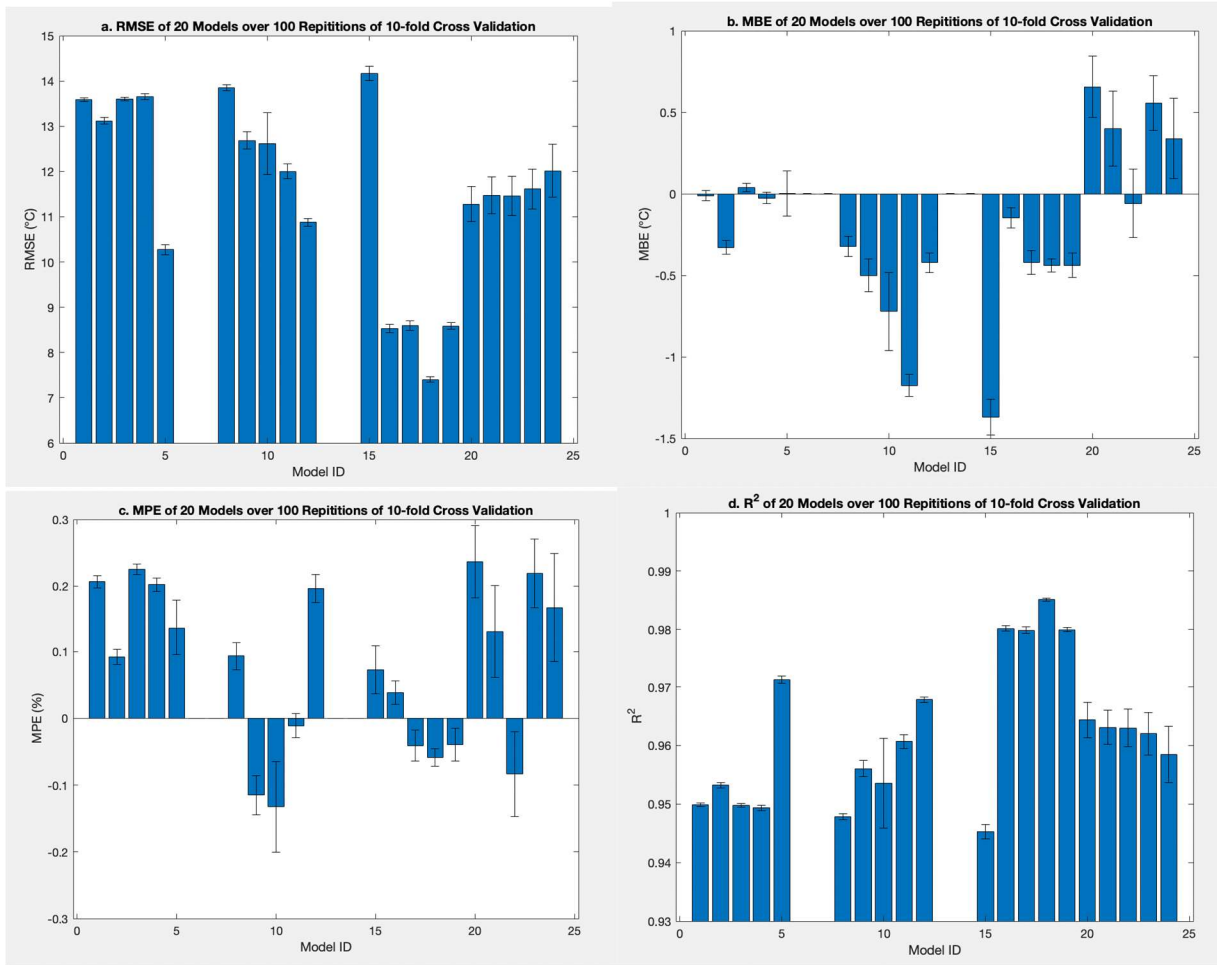


Figure 4

Comparison between the the 99 degree student-t 95% confidence intervals of a. RMSE b. MBE c. MPE and d. R².

As is demonstrated by the above performance metrics, there are various models with noteworthy predictive capabilities, particularly the GPR models (M16-M19), which had the highest mean R² and lowest mean RMSE values: all above 0.975 and below 9.0 respectively. The Exponential GPR model (M18) boasted an RMSE of 7.40 and and R² of 0.985, leading both the GPR and other models in these performance metrics.

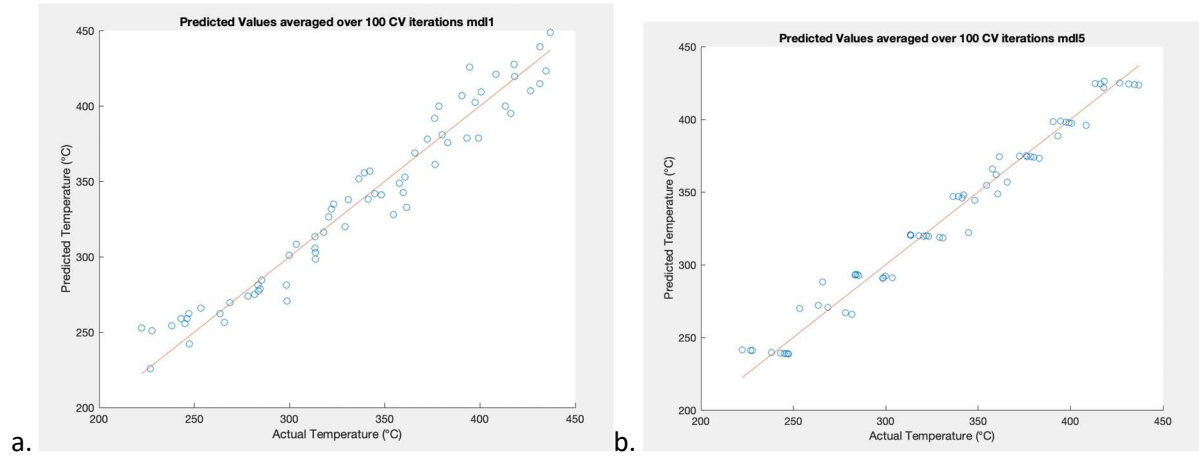
The Fine Tree (M5) and Medium Gaussian SVM (M12) lead in performance metrics after the GPR models, with a mean RMSE and R² of 10.27 and 0.971, and 10.87 and 0.968 respectively. The Neural Network models (M20-M24) had comparable metrics to one another, with the narrow neural network (M20) leading slightly with an RMSE of 11.28 and an R² of 0.964.

The basic linear regression machine learning model (M1) maintained good performance metrics with an RMSE of 13.58² and an R² of 0.950. Its metrics were comparable to that of the robust linear regression (M3) and stepwise linear regression (M4) models; while the interactions linear regression (M2) model had reduced RMSE and MPE, while increasing R², there was increased bias present in the model as made evident by the high MBE metric relative to the other linear regression models. Thus, without a definitive optimal linear regression model, we explore the basic linear regression (M1) model further for reference mostly, as its metrics are lacking compared to the other models selected for further analysis.

Boxplots of the performance metrics across all 100 repetitions for all the models can be found under Appendix B for RMSE, Appendix C for RRMSE, Appendix D for MBE, Appendix E for MPE, and Appendix F for R².

Fig. 5 shows the scattering of average predicted maximum temperature against the true maximum temperature for each biomass particle over the 100 repetitions of cross validation of the 8 models (M1,M5,M12,M16,M17,M18, M19, and M20) selected for further analysis (Lu,et.al)(Bagarello). Fig. 6 shows the corresponding residual plots for the 8 models (Hamidi).

Scatterplots of predicted against true maximum temperature for all 24 models can be found in Appendix G, and the residual plots for all 24 models can be found in Appendix H.



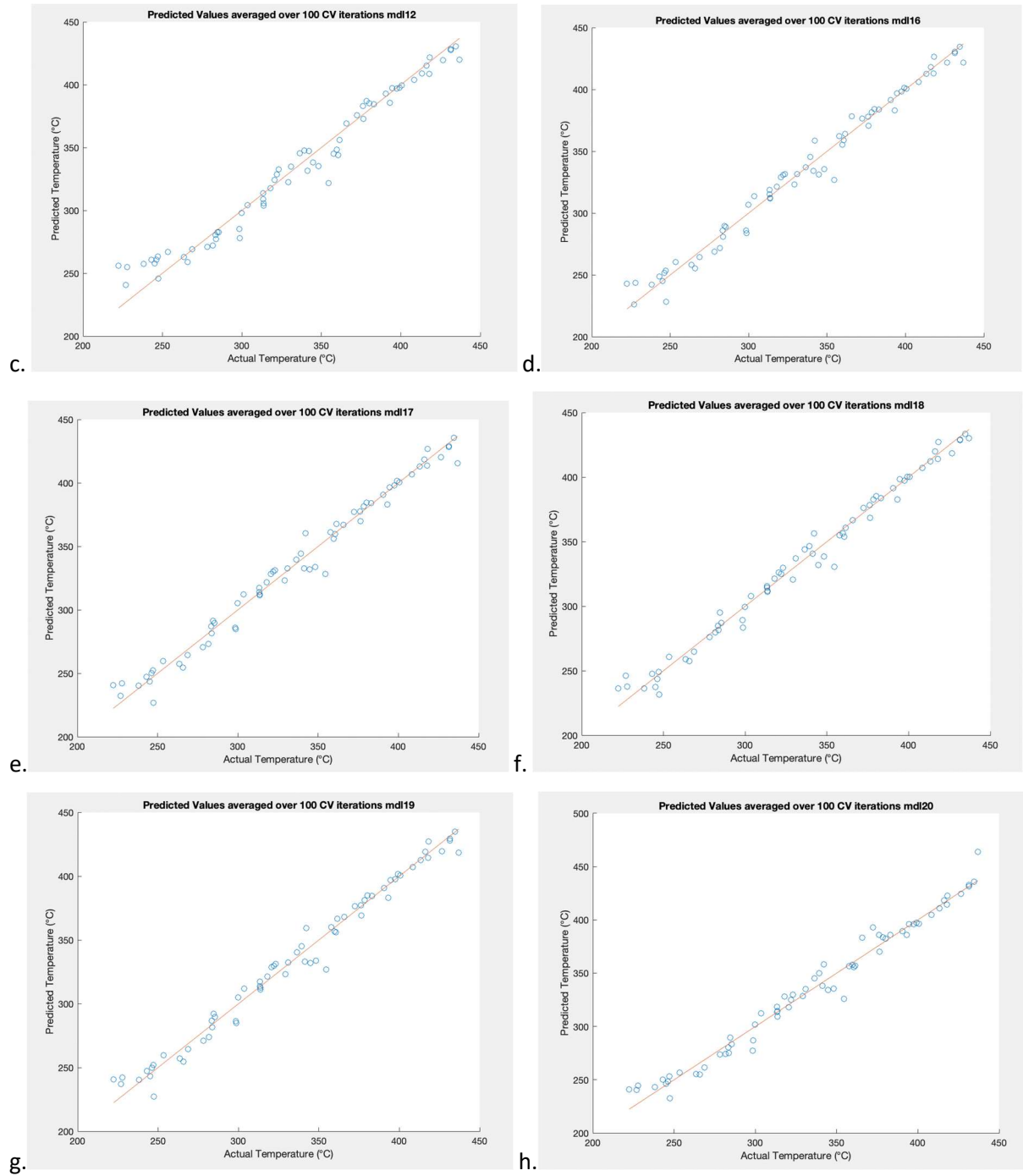
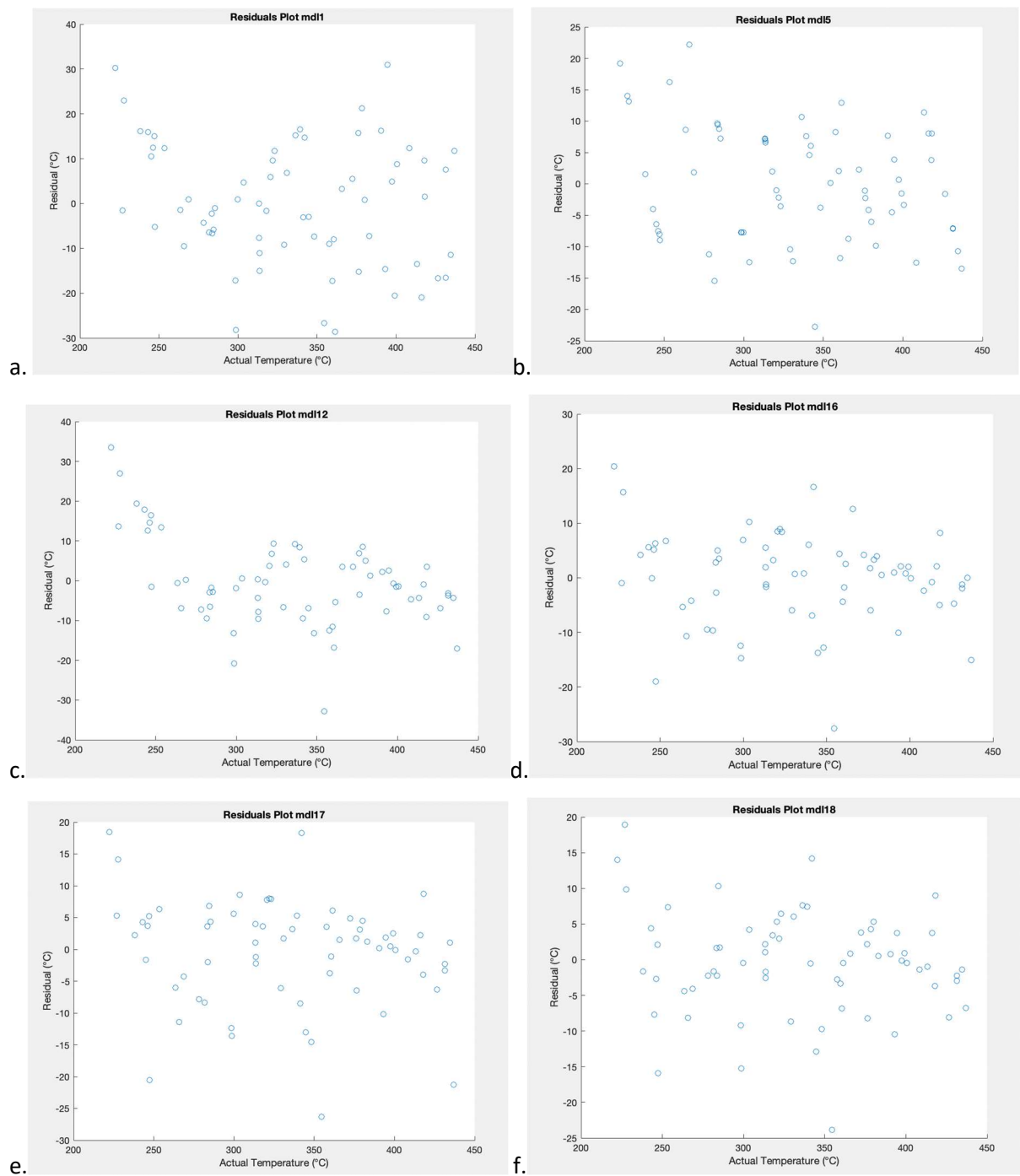


Figure 5

Comparison of the predicted maximum temperature plotted against the true maximum temperature (\square) experienced by the biomass particle during preparation for a. M1, b. M5, c. M12, d. M16, e. M17, f. M18, g. M19, and h. M20.



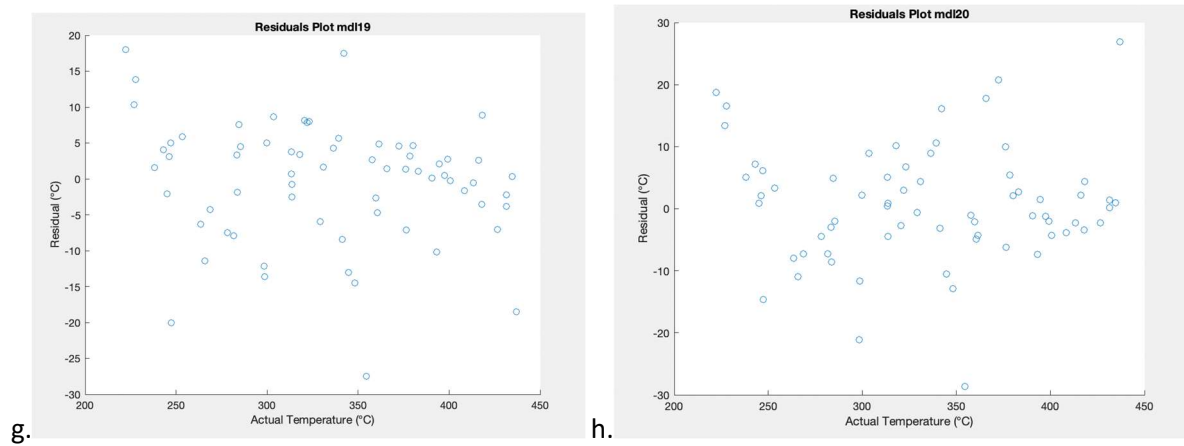


Figure 6

Model residuals of maximum temperature plotted against true maximum temperature (□) experienced by the biomass particle during preparation for a. M1, b. M5, c. M12, d. M16, e. M17, f. M18 g. M19. and h. M20.

From both the predicted and residual against actual temperature plots, we see a bias towards overestimation of maximum experienced temperature amongst biomass particles with the lowest actual maximum experienced temperature biomass particles for all models; however, this effect is less pronounced for Fig. 6.d.-g. the GPR models. This tendency is worth considering and may imply a lack of predictive capabilities far beyond the range of true maximum experienced temperatures. We also confirm through the tendency of temperature predictions to cluster that b. Fine Tree (M5) and other decision tree models are best utilized for categorical predictions like predicting best treatments (Sysoev).

3.3. Applying Models to Reactor-Prepared Biomass Particles

The GPR models (M16-M19) proved to have the best performance metrics, especially the Exponential GPR model (M18). Each model was trained using all 67 pieces of simulated biomass sample data, then all 4 models were utilized to predict the maximum temperature experienced by the approximately 30 biomass samples prepared in each of the 8 reactor conditions. The TG/DTG analysis plots of these biomass samples are found in appendix I, along with the tabular results of proximate analysis and thermochemical characteristics of the samples determined through TG/DTG analysis in appendix J.

The thermochemical characteristics and resulting biomass maximum temperature predictions for each of the 4 GPR models are reported in tables 3-10. The temperature prediction distribution histograms, along with the mean, standard deviation (Sd), skewness (Sk), and kurtosis (Kt) (Berg)(McKinnon) for each of the 8 reactor conditions are included in Fig. 7-14.

It is important to note that some characteristic features of these biomass samples fell outside of the ranges determined from the simulated samples whose maximum temperature experienced ranged from 222.4°C to 436.9°C. It is possible that some discrepancies between model predictions could be due to prediction errors occurring for biomass particles whose maximum experienced temperature occurred outside of this range and thus had characteristic features outside of the ranges from the simulated biomass samples. These ranges were 3.8 to 40.0 %/min, 377.2 to 510.8°C, and 0.0828 to 0.6245 for Rmax, Tmax, and FC proportion respectively. The 1122pine condition had around $\frac{1}{3}$ of its biomass samples with characteristics falling outside the simulated range, and thus the temperature distribution model predictions are likely least accurate for this condition. The other 7 conditions had a few biomass samples outside the characteristic ranges, but not nearly as many or with values as far outside the range as the 1122pine condition.

filenames	Rmax	Tmax	FCyield	finalramptemp16	finalramptemp17	finalramptemp18	finalramptemp19
20160227_run2_1125_pine_singleparticleanalysis.txt	37.3	387.97	0.1472	303.8	311	311.3	310.3
20160227_run5_1125_pine_singleparticleanalysis.txt	28.31	384.52	0.1344	250.7	232.5	254.8	233.4
20160227_run6_1125_pine_singleparticleanalysis.txt	28.78	390.6	0.0905	219.5	211.7	239.2	213.2
20160305_run1_1125_pine_singleparticleanalysis.txt	33.96	387.43	0.1378	280.5	285	288.8	285.2
20160306_run1_1125_pine_singleparticleanalysis.txt	6.28	456.54	0.5225	400.9	405.6	405	405.5
20160306_run3_1125_pine_singleparticleanalysis.txt	36.02	390.26	0.1445	294.8	306	307.6	306.6
20160306_run4_1125_pine_singleparticleanalysis.txt	31.37	394.6	0.0862	228.2	241.1	254.1	242.7
20160306_run5_1125_pine_singleparticleanalysis.txt	29.93	390.13	0.0988	231.4	220	238.3	217.7
20160306_run6_1125_pine_singleparticleanalysis.txt	34.22	390.69	0.1018	254.7	274.6	277.1	277.3
20160307_run2_1125_pine_singleparticleanalysis.txt	30.37	389.38	0.1301	256.5	240.4	253.1	237.1
20161207_run7_proxanalysis_20161125_pine_2dot6Lperm_sample1.txt	28.28	392.03	0.108	229.3	215	247.9	217.3
20161208_run1_proxanalysis_20161125_pine_2dot6Lperm_sample2.txt	30.39	387.96	0.1368	261.8	246.4	256.3	243.6
20170331_run1_20161125_sglpart_pine.txt	31.3	363.97	0.1014	247.8	295.1	279.8	305.2
20170331_run2_20161125_sglpart_pine.txt	5.69	350.69	0.4878	403.7	366	372.1	368
20170404_run1_20161125_sglpart_pine.txt	6.74	200	0.4274	409.1	365	354.5	365.6
20170404_run3_20161125_sglpart_pine.txt	37.18	362.09	0.1445	308.8	326.5	311	325.8
20170404_run4_20161125_sglpart_pine.txt	26.33	358.21	0.1008	224.3	302.4	283.3	311
20170404_run5_20161125_sglpart_pine.txt	21.35	360.16	0.2386	298.6	349.3	335	346.3
20170404_run6_20161125_sglpart_pine.txt	2.31	770.39	0.6766	401.2	365	389.1	373
20170404_run7_20161125_sglpart_pine.txt	28.91	368.46	0.0961	230.7	268.9	267.4	283.2
20170404_run8_20161125_sglpart_pine.txt	38.45	363.73	0.1146	293	318.9	303.8	319
20170405_run1_20161125_sglpart_pine.txt	5.37	420.29	0.5553	430.7	364.9	383.8	372.8
20170405_run2_20161125_sglpart_pine.txt	31.03	367.55	0.0874	235.2	279.1	269.4	291.1
20170405_run3_20161125_sglpart_pine.txt	24.91	363.75	0.1143	225.3	287.8	282.2	301.1
20170405_run4_20161125_sglpart_pine.txt	29.33	363.55	0.0839	225.4	286	272.1	298.1

Table 3 shows the thermochemical characteristics and resulting biomass maximum temperature predictions for each of the 4 GPR models for the 1125pine condition.

filenames	Rmax	Tmax	FCyield	finalramptemp16	finalramptemp17	finalramptemp18	finalramptemp19
20161026_run3_proxanalysis_20161023_pine_15SCFHtotal_sample1.txt	2.39	600.18	0.6841	456.6	367.2	413.7	384.8
20161026_run4_proxanalysis_20161023_pine_15SCFHtotal_sample2.txt	30.4	385.71	0.1655	283.3	281.7	290.3	284
20161026_run5_proxanalysis_20161023_pine_15SCFHtotal_sample3.txt	29.56	390.18	0.0992	229.8	217.2	238.4	215.3
20161026_run6_proxanalysis_20161023_pine_15SCFHtotal_sample4.txt	16.33	359.13	0.3636	364.3	373.3	365.9	369.1
20161026_run7_proxanalysis_20161023_pine_15SCFHtotal_sample5.txt	27.47	393.44	0.1085	225.2	215.5	253.4	222.2
20161026_run8_proxanalysis_20161023_pine_15SCFHtotal_sample6.txt	23.18	376.11	0.3304	369.5	368.9	367	367.5
20161026_run9_proxanalysis_20161023_pine_15SCFHtotal_sample7.txt	30.19	386.45	0.1236	251.7	233.2	237.7	229.6
20161028_run3_proxanalysis_20161023_pine_15SCFHtotal_sample8.txt	35.02	389.15	0.1432	289.1	297.8	301.3	298.6
20161028_run4_proxanalysis_20161023_pine_15SCFHtotal_sample9.txt	35.48	383.71	0.1762	317	322.6	322.5	324.2
20161028_run5_proxanalysis_20161023_pine_15SCFHtotal_sample10.txt	4.56	529.08	0.5339	379.5	406.3	424.3	412.2
20161028_run7_proxanalysis_20161023_pine_15SCFHtotal_sample12.txt	4.11	451.79	0.5234	392.1	405.3	402.3	405
20161028_run8_proxanalysis_20161023_pine_15SCFHtotal_sample13.txt	39.07	384.21	0.1879	343.2	334.1	335.7	335.1
20161029_run2_proxanalysis_20161023_pine_15SCFHtotal_sample14.txt	21.77	372.26	0.323	358.2	367.9	363.9	365.5
20161029_run3_proxanalysis_20161023_pine_15SCFHtotal_sample15.txt	27.17	374.4	0.2789	352.6	364	357.1	361.1
20161029_run4_proxanalysis_20161023_pine_15SCFHtotal_sample16.txt	35.17	389.44	0.1146	269.1	287.4	290.4	289.8
20161029_run5_proxanalysis_20161023_pine_15SCFHtotal_sample17.txt	36.75	389.73	0.1671	314.9	319.9	317.4	319.5
20161029_run6_proxanalysis_20161023_pine_15SCFHtotal_sample18.txt	28.53	388.51	0.1125	234.8	214.7	241.6	214
20161029_run7_proxanalysis_20161023_pine_15SCFHtotal_sample19.txt	33.98	382.7	0.1839	315.3	327.8	330.1	332.1
20161029_run8_proxanalysis_20161023_pine_15SCFHtotal_sample20.txt	31.09	387.49	0.1142	249.1	236.3	239.5	232.5
20161030_run1_proxanalysis_20161023_pine_15SCFHtotal_sample21.txt	31.32	390	0.09	232	233.3	242.9	231.7
20161030_run5_proxanalysis_20161023_pine_15SCFHtotal_sample22.txt	19.78	370.43	0.3581	374.2	373.6	370	371
20161030_run6_proxanalysis_20161023_pine_15SCFHtotal_sample23.txt	3.6	509.01	0.4775	339.7	407.1	420.2	412.1
20161030_run7_proxanalysis_20161023_pine_15SCFHtotal_sample24.txt	30.45	389.09	0.1653	282.4	279.6	291.1	281.3
20161030_run8_proxanalysis_20161023_pine_15SCFHtotal_sample25.txt	14.11	367.73	0.4353	402.6	374	375.1	372.7
20161031_run1_proxanalysis_20161023_pine_15SCFHtotal_sample26.txt	35.14	386.7	0.1569	300.4	306.2	306.4	306.6
20161031_run1_proxanalysis_20161023_pine_15SCFHtotal_sample27.txt	9.43	357.91	0.3933	351.8	369.7	365.7	367.4
20161031_run3_proxanalysis_20161023_pine_15SCFHtotal_sample28.txt	3.78	468.84	0.6055	444.9	423.4	422.8	423
20161031_run4_proxanalysis_20161023_pine_15SCFHtotal_sample29.txt	35.96	388.31	0.1476	297.3	305.1	305.7	305
20161031_run5_proxanalysis_20161023_pine_15SCFHtotal_sample30.txt	28.18	387.97	0.0912	217.8	208	237	210.8

Table 4 shows the thermochemical characteristics and resulting biomass maximum temperature predictions for each of the 4 GPR models for the 20161023_pine_15scfhtotal_table condition.

filenames	Rmax	Tmax	FCyield	finalramptemp16	finalramptemp17	finalramptemp18	finalramptemp19
1126pine							
20160227_run1_1126_pine_singleparticleanalysis.txt	31.08	382.68	0.1169	252.4	242.2	233.7	241.2
20161130_run2_proxanalysis_20161126_pine_2dot0Lperm_sample1.txt	9.88	380.01	0.424	369.8	369	371.8	369.3
20161130_run3_proxanalysis_20161126_pine_2dot0Lperm_sample2.txt	37.7	392.74	0.1135	280	313.5	307.3	316.9
20161201_run5_proxanalysis_20161126_pine_2dot0Lperm_sample3.txt	36.19	389.36	0.149	299.2	308	308.9	308.1
20161202_run1_proxanalysis_20161126_pine_2dot0Lperm_sample4.txt	31.41	391.63	0.1016	240.4	238.5	250.2	236.7
20161202_run2_proxanalysis_20161126_pine_2dot0Lperm_sample5.txt	30.39	389.82	0.0802	220.3	223.2	237.5	222.8
20161202_run3_proxanalysis_20161126_pine_2dot0Lperm_sample6.txt	33.41	378.7	0.2031	327.5	345.6	342.1	350.6
20161202_run4_proxanalysis_20161126_pine_2dot0Lperm_sample7.txt	29.72	395.08	0.0773	213.3	226.4	248.4	230.8
20161202_run5_proxanalysis_20161126_pine_2dot0Lperm_sample8.txt	32.04	388.75	0.1255	261.7	255.4	261.2	253.2
20161202_run6_proxanalysis_20161126_pine_2dot0Lperm_sample9.txt	33.01	391.33	0.1341	271.9	275	282.2	275.4
20161203_run2_proxanalysis_20161126_pine_2dot0Lperm_sample10.txt	30.46	390.16	0.0923	229.3	224	238.7	222
20161203_run3_proxanalysis_20161126_pine_2dot0Lperm_sample11.txt	26.37	392.96	0.0764	196.6	212.5	249	227.3
20161203_run4_proxanalysis_20161126_pine_2dot0Lperm_sample12.txt	32.64	393.22	0.113	254.3	261	269.3	261.6
20161203_run5_proxanalysis_20161126_pine_2dot0Lperm_sample13.txt	29.46	395.18	0.1208	243.5	234.1	260.8	235.5
20161204_run3_proxanalysis_20161126_pine_2dot0Lperm_sample14.txt	33.09	393.8	0.1105	254.5	266.7	273.2	268.5
20161204_run4_proxanalysis_20161126_pine_2dot0Lperm_sample15.txt	32.64	393.71	0.1177	257.5	263.9	272.5	264.8
20161204_run5_proxanalysis_20161126_pine_2dot0Lperm_sample16.txt	29.22	387.68	0.0633	202.9	217.6	235.4	221.9
20161204_run6_proxanalysis_20161126_pine_2dot0Lperm_sample17.txt	34.89	389.05	0.1769	313	321.2	322.4	322.8
20161204_run7_proxanalysis_20161126_pine_2dot0Lperm_sample18.txt	32.89	391.55	0.1096	253.5	260.4	267.1	260.8
20161205_run2_proxanalysis_20161126_pine_2dot0Lperm_sample19.txt	29.26	394.28	0.0931	222.7	221	248.1	223.7
20161205_run3_proxanalysis_20161126_pine_2dot0Lperm_sample20.txt	29.82	388.96	0.1286	252.8	233.8	249.4	230.5
20161205_run4_proxanalysis_20161126_pine_2dot0Lperm_sample21.txt	35.38	393.84	0.1728	311.1	320.9	320.3	321.3
20161205_run5_proxanalysis_20161126_pine_2dot0Lperm_sample22.txt	39.39	394.22	0.1399	307.1	328.6	322	329.2
20161206_run3_proxanalysis_20161126_pine_2dot0Lperm_sample25.txt	32.58	391.05	0.0924	239.7	251.2	257	251.6
20161206_run4_proxanalysis_20161126_pine_2dot0Lperm_sample26.txt	30.23	388.04	0.2331	330.7	344.7	346	347.8
20161206_run6_proxanalysis_20161126_pine_2dot0Lperm_sample27.txt	32.95	390.65	0.1543	286.4	290.5	296.3	291.9
20161207_run2_proxanalysis_20161126_pine_2dot0Lperm_sample28.txt	33.65	389.92	0.1458	284	289.2	294.5	290.2
20161207_run3_proxanalysis_20161126_pine_2dot0Lperm_sample29.txt	27.33	393.06	0.0857	208.1	211.1	247.2	220.7
20161207_run4_proxanalysis_20161126_pine_2dot0Lperm_sample30.txt	30.35	390.49	0.0862	224.3	223.1	238.9	222

Table 5 shows the thermochemical characteristics and resulting biomass maximum temperature predictions for each of the 4 GPR models for the 1126pine condition.

filenames	Rmax	Tmax	FCyield	finalramptemp16	finalramptemp17	finalramptemp18	finalramptemp19
20161026_run3_proxanalysis_20161023_pine_15SCFHtotal_sample1.txt	2.39	600.18	0.6841	456.6	367.2	413.7	384.8
20161026_run4_proxanalysis_20161023_pine_15SCFHtotal_sample2.txt	30.4	385.71	0.1655	283.3	281.7	290.3	284
20161026_run5_proxanalysis_20161023_pine_15SCFHtotal_sample3.txt	29.56	390.18	0.0992	229.8	217.2	238.4	215.3
20161026_run6_proxanalysis_20161023_pine_15SCFHtotal_sample4.txt	16.33	359.13	0.3636	364.3	373.3	365.9	369.1
20161026_run7_proxanalysis_20161023_pine_15SCFHtotal_sample5.txt	27.47	393.44	0.1085	225.2	215.5	253.4	222.2
20161026_run8_proxanalysis_20161023_pine_15SCFHtotal_sample6.txt	23.18	376.11	0.3304	369.5	368.9	367	367.5
20161026_run9_proxanalysis_20161023_pine_15SCFHtotal_sample7.txt	30.19	386.45	0.1236	251.7	233.2	237.7	229.6
20161028_run3_proxanalysis_20161023_pine_15SCFHtotal_sample8.txt	35.02	389.15	0.1432	289.1	297.8	301.3	298.6
20161028_run4_proxanalysis_20161023_pine_15SCFHtotal_sample9.txt	35.48	383.71	0.1762	317	322.6	322.5	324.2
20161028_run5_proxanalysis_20161023_pine_15SCFHtotal_sample10.txt	4.56	529.08	0.5339	379.5	406.3	424.3	412.2
20161028_run7_proxanalysis_20161023_pine_15SCFHtotal_sample12.txt	4.11	451.79	0.5234	392.1	405.3	402.3	405
20161028_run8_proxanalysis_20161023_pine_15SCFHtotal_sample13.txt	39.07	384.21	0.1879	343.2	334.1	335.7	335.1
20161029_run2_proxanalysis_20161023_pine_15SCFHtotal_sample14.txt	21.77	372.26	0.323	358.2	367.9	363.9	365.5
20161029_run3_proxanalysis_20161023_pine_15SCFHtotal_sample15.txt	27.17	374.4	0.2789	352.6	364	357.1	361.1
20161029_run4_proxanalysis_20161023_pine_15SCFHtotal_sample16.txt	35.17	389.44	0.1146	269.1	287.4	290.4	289.8
20161029_run5_proxanalysis_20161023_pine_15SCFHtotal_sample17.txt	36.75	389.73	0.1671	314.9	319.9	317.4	319.5
20161029_run6_proxanalysis_20161023_pine_15SCFHtotal_sample18.txt	28.53	388.51	0.1125	234.8	214.7	241.6	214
20161029_run7_proxanalysis_20161023_pine_15SCFHtotal_sample19.txt	33.98	382.7	0.1839	315.3	327.8	330.1	332.1
20161029_run8_proxanalysis_20161023_pine_15SCFHtotal_sample20.txt	31.09	387.49	0.1142	249.1	236.3	239.5	232.5
20161030_run4_proxanalysis_20161023_pine_15SCFHtotal_sample21.txt	31.32	390	0.09	232	233.3	242.9	231.7
20161030_run5_proxanalysis_20161023_pine_15SCFHtotal_sample22.txt	19.78	370.43	0.3581	374.2	373.6	370	371
20161030_run6_proxanalysis_20161023_pine_15SCFHtotal_sample23.txt	3.6	509.01	0.4775	339.7	407.1	420.2	412.1
20161030_run7_proxanalysis_20161023_pine_15SCFHtotal_sample24.txt	30.45	389.09	0.1653	282.4	279.6	291.1	281.3
20161030_run8_proxanalysis_20161023_pine_15SCFHtotal_sample25.txt	14.11	367.73	0.4353	402.6	374	375.1	372.7
20161031_run1_proxanalysis_20161023_pine_15SCFHtotal_sample26.txt	35.14	386.7	0.1569	300.4	306.2	306.4	306.6
20161031_run2_proxanalysis_20161023_pine_15SCFHtotal_sample27.txt	9.43	357.91	0.3933	351.8	369.7	365.7	367.4
20161031_run3_proxanalysis_20161023_pine_15SCFHtotal_sample28.txt	3.78	468.84	0.6055	444.9	423.4	422.8	423
20161031_run4_proxanalysis_20161023_pine_15SCFHtotal_sample29.txt	35.96	388.31	0.1476	297.3	305.1	305.7	305
20161031_run5_proxanalysis_20161023_pine_15SCFHtotal_sample30.txt	28.18	387.97	0.0912	217.8	208	237	210.8

Table 6 shows the thermochemical characteristics and resulting biomass maximum temperature predictions for each of the 4 GPR models for the 20161023_pine_15scfhtotal condition.

filenames	Rmax	Tmax	FCyield	finalramptemp16	finalramptemp17	finalramptemp18	finalramptemp19
2016105_run7_proxanalysis_20161025_pine_20SCFHtotal_sample1.txt	34.84	389.25	0.1624	302.1	309.8	311.5	311
2016105_run8_proxanalysis_20161025_pine_20SCFHtotal_sample2.txt	28.53	391.58	0.0822	212	212	241.1	216.3
2016106_run10_proxanalysis_20161025_pine_20SCFHtotal_sample12.txt	13.7	378.56	0.3915	365.8	374.4	374	374.7
2016106_run11_proxanalysis_20161025_pine_20SCFHtotal_sample3.txt	36.19	391.17	0.1359	289.1	304.8	306.3	306.3
2016106_run2_proxanalysis_20161025_pine_20SCFHtotal_sample4.txt	31.74	393.09	0.0993	239.9	244.5	255.9	244.2
2016106_run3_proxanalysis_20161025_pine_20SCFHtotal_sample5.txt	26.74	389.66	0.1005	216.8	208.8	248.1	217.7
2016106_run4_proxanalysis_20161025_pine_20SCFHtotal_sample6.txt	36.6	389.81	0.1412	295.4	307.4	308.7	307.8
2016106_run5_proxanalysis_20161025_pine_20SCFHtotal_sample7.txt	29.91	387.19	0.1666	281.2	277.7	289.8	279.8
2016106_run7_proxanalysis_20161025_pine_20SCFHtotal_sample9.txt	28.94	386.58	0.0922	222.8	211.4	232.2	211.4
2016106_run8_proxanalysis_20161025_pine_20SCFHtotal_sample10.txt	36.54	384.85	0.1562	307.4	309.9	307.2	308.8
2016106_run9_proxanalysis_20161025_pine_20SCFHtotal_sample11.txt	35.26	388.62	0.1774	315.2	322.5	323.2	323.8
2016107_run2_proxanalysis_20161025_pine_20SCFHtotal_sample13.txt	30.9	393.24	0.1097	243.2	238	254.5	236.7
2016107_run3_proxanalysis_20161025_pine_20SCFHtotal_sample14.txt	27.87	391.86	0.1003	221.8	211.3	246.4	215.8
2016107_run4_proxanalysis_20161025_pine_20SCFHtotal_sample15.txt	24.55	390.76	0.1221	221.3	224.9	267.3	242.5
2016107_run5_proxanalysis_20161025_pine_20SCFHtotal_sample16.txt	25.74	381.89	0.2873	349.3	358.8	359.2	359
2016107_run6_proxanalysis_20161025_pine_20SCFHtotal_sample17.txt	26.61	390.08	0.1132	225.3	213.2	253.5	221.7
2016107_run7_proxanalysis_20161025_pine_20SCFHtotal_sample18.txt	27.62	388.74	0.0923	215.6	207.1	240.7	212.4
2016108_run3_proxanalysis_20161025_pine_20SCFHtotal_sample19.txt	37.6	395.34	0.1527	307.1	323.4	319.2	323.3
2016108_run4_proxanalysis_20161025_pine_20SCFHtotal_sample20.txt	26.85	388.22	0.1062	222	209.7	247.8	217.1
2016109_run1_proxanalysis_20161025_pine_20SCFHtotal_sample21.txt	36.55	392.02	0.156	305.2	315.8	315.1	315.9
2016109_run2_proxanalysis_20161025_pine_20SCFHtotal_sample22.txt	29.09	388.41	0.0789	213.4	212.6	234.3	214.4
2016109_run3_proxanalysis_20161025_pine_20SCFHtotal_sample23.txt	30.73	390.18	0.1465	269.9	260.3	273	259.2
2016109_run4_proxanalysis_20161025_pine_20SCFHtotal_sample24.txt	39.53	390.03	0.1554	320.2	326.7	327.1	326.6
2016109_run5_proxanalysis_20161025_pine_20SCFHtotal_sample25.txt	33.99	390.2	0.108	258.3	272.7	276.7	274.6
2016109_run6_proxanalysis_20161025_pine_20SCFHtotal_sample28.txt	37.86	392.82	0.1388	299.1	318.1	315.8	319.1
2016110_run5_proxanalysis_20161025_pine_20SCFHtotal_sample27.txt	6.13	445.31	0.497	385	392.6	392.7	393.1
2016111_run2_proxanalysis_20161025_pine_20SCFHtotal_sample29.txt	36.45	391.8	0.1491	299.8	312.1	312.4	312.7
2016111_run3_proxanalysis_20161025_pine_20SCFHtotal_sample30.txt	37.82	383.65	0.1645	320.2	318.2	315.9	317.2

Table 7 shows the thermochemical characteristics and resulting biomass maximum temperature predictions for each of the 4 GPR models for the 20161025_pine_20scfhtotal_table condition.

filenames	Rmax	Tmax	FCyield	finalramptemp16	finalramptemp17	finalramptemp18	finalramptemp19
20161111_run4_proxanalysis_20161107_pine_15SCFHTotal_sample1.txt	36.03	390.48	0.1737	315.9	322.2	321	322.3
20161111_run5_proxanalysis_20161107_pine_15SCFHTotal_sample2.txt	34.31	389.12	0.1869	317.3	327.4	329.6	329.9
20161111_run6_proxanalysis_20161107_pine_15SCFHTotal_sample3.txt	34.72	387.63	0.1937	324.6	334	336.6	336.4
20161112_run1_proxanalysis_20161107_pine_15SCFHTotal_sample4.txt	28.1	388.62	0.1383	251.3	232.3	260.9	233.5
20161112_run2_proxanalysis_20161107_pine_15SCFHTotal_sample5.txt	33.86	387.43	0.1564	293.5	299.1	302.1	300.4
20161112_run3_proxanalysis_20161107_pine_15SCFHTotal_sample6.txt	24.26	381.69	0.2539	317.8	341.2	344.3	344.8
20161112_run4_proxanalysis_20161107_pine_15SCFHTotal_sample7.txt	30.64	391.01	0.1044	238.8	229.5	244.4	226.7
20161112_run5_proxanalysis_20161107_pine_15SCFHTotal_sample8.txt	34.22	391.3	0.1002	253.4	275	277	278
20161112_run6_proxanalysis_20161107_pine_15SCFHTotal_sample9.txt	2.57	589.37	0.6242	417.3	369.1	414.5	387.1
20161112_run7_proxanalysis_20161107_pine_15SCFHTotal_sample10.txt	14.8	374.26	0.2112	242	332.5	326.9	336.9
20161113_run1_proxanalysis_20161107_pine_15SCFHTotal_sample11.txt	2.49	637.25	0.6899	450.5	365.3	406.5	379.7
20161113_run2_proxanalysis_20161107_pine_15SCFHTotal_sample12.txt	6.55	200.1	0.4469	422.2	365	355.3	365.8
20161113_run3_proxanalysis_20161107_pine_15SCFHTotal_sample13.txt	26.76	389.74	0.1009	217.2	208.7	248	217.5
20161113_run4_proxanalysis_20161107_pine_15SCFHTotal_sample14.txt	2.01	604.17	0.6661	440.5	366.8	412.5	384.1
20161113_run5_proxanalysis_20161107_pine_15SCFHTotal_sample15.txt	35.87	388.16	0.1528	300.6	307.4	307.7	307.3
20161113_run6_proxanalysis_20161107_pine_15SCFHTotal_sample16.txt	26.64	387.12	0.1117	225.2	212.4	250.5	220.3
20161114_run1_proxanalysis_20161107_pine_15SCFHTotal_sample17.txt	32.54	388.68	0.095	242.1	248.8	253.1	248.2
20161114_run3_proxanalysis_20161107_pine_15SCFHTotal_sample18.txt	3.97	469.24	0.4833	357.3	409.5	410.2	409.4
20161115_run2_proxanalysis_20161107_pine_15SCFHTotal_sample19.txt	32.51	386.61	0.174	299.7	308.3	312.6	312.2
20161115_run3_proxanalysis_20161107_pine_15SCFHTotal_sample20.txt	26.01	388.07	0.2289	306.6	322.8	332.2	328.7
20161115_run4_proxanalysis_20161107_pine_15SCFHTotal_sample21.txt	34.77	391.04	0.1346	281.1	293.1	298.4	294.7
20161115_run5_proxanalysis_20161107_pine_15SCFHTotal_sample22.txt	27.16	387.25	0.2204	306.4	320.8	329.3	326.6
20161117_run2_proxanalysis_20161107_pine_15SCFHTotal_sample23.txt	32.25	391.37	0.1298	265	263	271.8	262.2
20161117_run4_proxanalysis_20161107_pine_15SCFHTotal_sample24.txt	27.01	392.08	0.0961	214.3	210	248.7	219.1
20161118_run4_proxanalysis_20161107_pine_15SCFHTotal_sample25.txt	29.97	392.55	0.1053	235.6	225.6	247.3	224.2
20161119_run3_proxanalysis_20161107_pine_15SCFHTotal_sample26.txt	34.27	387.47	0.1544	294	299.9	302.3	300.9
20161119_run5_proxanalysis_20161107_pine_15SCFHTotal_sample27.txt	28.47	386.88	0.085	215.1	209.2	234.2	211.9
20161119_run6_proxanalysis_20161107_pine_15SCFHTotal_sample28.txt	38.87	389.35	0.1761	332.1	330.1	324.6	329.5
20161120_run5_proxanalysis_20161107_pine_15SCFHTotal_sample29.txt	1.16	374.88	0.7499	563.8	364.5	390.8	374.4
20161120_run6_proxanalysis_20161107_pine_15SCFHTotal_sample30.txt	25.79	390.04	0.0982	210.4	210.7	252.3	224.7

Table 8 shows the thermochemical characteristics and resulting biomass maximum temperature predictions for each of the 4 GPR models for the 20161107 condition.

1120pine

filenames	Rmax	Tmax	FCyield	finalramptemp16	finalramptemp17	finalramptemp18	finalramptemp19
20161120_run7_proxanalysis_20161120_pine_8dot7SCFHtotal_sample1.txt	2.75	200.21	0.5953	510.7	365	361.5	366.9
20161120_run8_proxanalysis_20161120_pine_8dot7SCFHtotal_sample2.txt	18.66	379.4	0.2996	323.7	356.7	356.5	357.1
20161122_run3C_proxanalysis_20161120_pine_8dot7SCFHtotal_sample3C.txt	28.69	385.08	0.1503	264	250.7	269.3	251.9
20161122_run4_proxanalysis_20161120_pine_8dot7SCFHtotal_sample4.txt	24.84	386.67	0.1567	249	250.5	284.2	264.1
20161122_run5_proxanalysis_20161120_pine_8dot7SCFHtotal_sample5.txt	5.3	451.83	0.4785	365.5	400.1	397.6	400.3
20161123_run3_proxanalysis_20161120_pine_8dot7SCFHtotal_sample12.txt	26.39	392.85	0.1015	214.9	212.7	253.8	224.6
20161123_run3_proxanalysis_20161120_pine_8dot7SCFHtotal_sample6.txt	33.73	392.4	0.1023	252.2	270.6	274	273.1
20161123_run4_proxanalysis_20161120_pine_8dot7SCFHtotal_sample13.txt	30.91	387.93	0.119	251.6	237.1	242.3	233.3
20161123_run5_proxanalysis_20161120_pine_8dot7SCFHtotal_sample7.txt	4.01	471.41	0.6123	450.2	424.2	424.1	423.7
20161123_run5_proxanalysis_20161120_pine_8dot7SCFHtotal_sample8.txt	23.43	392.15	0.0991	198.6	225.4	264.7	248.6
20161123_run7_proxanalysis_20161120_pine_8dot7SCFHtotal_sample9.txt	14.2	380.35	0.4433	405.2	372.6	376.9	373
20161123_run8_proxanalysis_20161120_pine_8dot7SCFHtotal_sample10.txt	25.51	385.57	0.12	226.1	220.8	260.1	233.8
20161124_run2_proxanalysis_20161120_pine_8dot7SCFHtotal_sample11.txt	2.76	558.61	0.705	485.7	380.6	423.9	396.8
20170406_run2_20161120_sgpart_pine.txt	30.52	361.69	0.1241	260.9	307.6	289.7	315.4
20170406_run3_20161120_sgpart_pine.txt	33.56	367.86	0.1136	266.7	297	285.9	304.4
20170406_run4_20161120_sgpart_pine.txt	4.85	435.27	0.5269	403.2	380.3	385.8	381.7
20170406_run5_20161120_sgpart_pine.txt	40.56	364.5	0.1553	332.7	331.4	320.9	331
20170406_run6_20161120_sgpart_pine.txt	33.69	362.84	0.1029	261	306.4	287.3	312.4
20170406_run7_20161120_sgpart_pine.txt	2.94	597.96	0.5905	392.3	367.6	411.5	384.9
20170407_run1_20161120_sgpart_pine.txt	34.2	359.6	0.1079	268.2	316.1	293.1	319.4
20170407_run2_20161120_sgpart_pine.txt	33.8	362.35	0.0889	251.6	305.2	283.9	311.1
20170407_run3_20161120_sgpart_pine.txt	29.53	368.85	0.0999	236.4	270.8	268.6	284.3
20170408_run1_20161120_sgpart_pine.txt	31.97	363.85	0.1004	250.4	297.5	281.1	306.7
20170408_run2_20161120_sgpart_pine.txt	24.15	338.48	0.2966	360.8	368.4	348.2	358.6
20170409_run1_20161120_sgpart_pine.txt	31.12	364.22	0.088	237.1	290.4	274.8	301.1
20170409_run2_20161120_sgpart_pine.txt	33.06	370.33	0.0959	250.6	282.9	274.5	292.1
20170409_run3_20161120_sgpart_pine.txt	5.58	427.3	0.5312	412.2	369.6	382	373.5
20170409_run4_20161120_sgpart_pine.txt	34.5	359.92	0.1624	309	335.5	313.7	334.4
20170409_run5_20161120_sgpart_pine.txt	32.74	364.55	0.1211	269	305.4	289.9	312.7
20170410_run1_20161120_sgpart_pine.txt	32.07	370.28	0.1027	250.7	279.4	273.4	289.8
20170410_run3_20161120_sgpart_pine.txt	34.55	364.14	0.1289	283.7	313.9	298	317.5

Table 9 shows the thermochemical characteristics and resulting biomass maximum temperature predictions for each of the 4 GPR models for the 1120pine condition.

filenames	Rmax	Tmax	FCyield	finalramptemp16	finalramptemp17	finalramptemp18	finalramptemp19
20161123_run5_proxanalysis_20161122_pine_21SCFHtotal_sample1.txt	30.24	387.41	0.1657	282.2	279.2	290.1	281.1
20161123_run6_proxanalysis_20161122_pine_21SCFHtotal_sample2.txt	4.55	200.04	0.5823	510.3	365	360.9	366.7
20161124_run7_proxanalysis_20161122_pine_21SCFHtotal_sample3.txt	24.25	389.7	0.1353	229.7	233.9	274.3	251.5
20161124_run8_proxanalysis_20161122_pine_21SCFHtotal_sample4.txt	23.75	389.73	0.0709	180.5	222.6	256.1	246
20161125_run2_proxanalysis_20161122_pine_21SCFHtotal_sample5.txt	16.62	388.24	0.3181	324.3	359.6	359.9	360.4
20161125_run3_proxanalysis_20161122_pine_21SCFHtotal_sample6.txt	27.24	390.27	0.152	256.4	244.1	276	249.6
20161125_run4_proxanalysis_20161122_pine_21SCFHtotal_sample7.txt	18.84	385.82	0.1488	213.6	278.8	296.7	298.8
20161125_run5_proxanalysis_20161122_pine_21SCFHtotal_sample8.txt	22.99	381.61	0.1709	251.5	274.7	297.9	290.4
20161125_run6_proxanalysis_20161122_pine_21SCFHtotal_sample9.txt	5.93	447.23	0.5129	394.9	395.3	394.2	395.4
20161125_run7_proxanalysis_20161122_pine_21SCFHtotal_sample10.txt	30.1	391.23	0.1231	249.5	233.9	252.3	231.1
20161125_run8_proxanalysis_20161122_pine_21SCFHtotal_sample11.txt	6.08	200.18	0.3852	375.2	365	352.7	365.4
20161126_run2_proxanalysis_20161122_pine_21SCFHtotal_sample12.txt	22.82	387.18	0.0947	193.8	228.6	264.1	252.9
20161126_run3_proxanalysis_20161122_pine_21SCFHtotal_sample13.txt	2.2	200.2	0.7159	595.2	365	365.7	367.6
20161126_run4_proxanalysis_20161122_pine_21SCFHtotal_sample14.txt	23.28	389.16	0.1738	252.9	269.2	298.4	285.4
20161126_run5_proxanalysis_20161122_pine_21SCFHtotal_sample15.txt	2.24	604.87	0.7411	495.8	366.5	413.6	383.8
20161126_run6_proxanalysis_20161122_pine_21SCFHtotal_sample16.txt	2.79	608.92	0.6228	411.7	366.5	410.3	383.2
20161126_run7_proxanalysis_20161122_pine_21SCFHtotal_sample17.txt	29.6	394.41	0.118	242.4	231.9	257.5	232.3
20161126_run8_proxanalysis_20161122_pine_21SCFHtotal_sample18.txt	24.77	392.77	0.1483	240.7	243	281.4	258.5
20161127_run2_proxanalysis_20161122_pine_21SCFHtotal_sample19.txt	24.04	382.62	0.2614	321.9	344.2	347.4	347.4
20161127_run4_proxanalysis_20161122_pine_21SCFHtotal_sample20.txt	3.44	200.16	0.6698	568.1	365	364.1	367.3
20161127_run5_proxanalysis_20161122_pine_21SCFHtotal_sample21.txt	1.44	642	0.7342	475.9	365.2	406.4	379.2
20161127_run6_proxanalysis_20161122_pine_21SCFHtotal_sample22.txt	6.04	444.92	0.5107	394.5	392	391.6	392.2
20161127_run7_proxanalysis_20161122_pine_21SCFHtotal_sample23.txt	3.71	515.35	0.499	353.9	409.8	422.9	414.3
20161127_run8_proxanalysis_20161122_pine_21SCFHtotal_sample24.txt	30.78	387.53	0.1713	288.9	290.7	299.1	293.7
20161128_run2_proxanalysis_20161122_pine_21SCFHtotal_sample25.txt	2.44	564.6	0.6141	416.5	378.5	420.2	394.9
20161128_run3_proxanalysis_20161122_pine_21SCFHtotal_sample26.txt	22.29	387.06	0.1761	250.2	275.5	301.4	292.4
20161128_run6_proxanalysis_20161122_pine_21SCFHtotal_sample27.txt	17.46	390.83	0.2525	280.3	334.7	339.2	340.5
20161128_run8_proxanalysis_20161122_pine_21SCFHtotal_sample28.txt	37.48	386.07	0.2276	363.4	347.7	344.1	344.8
20161129_run3_proxanalysis_20161122_pine_21SCFHtotal_sample29.txt	2.84	200.2	0.7052	590.7	365	365.3	367.5
20161129_run4_proxanalysis_20161122_pine_21SCFHtotal_sample30.txt	2.38	450.34	0.592	433.6	405.7	408.1	406.6

Table 10 shows the thermochemical characteristics and resulting biomass maximum temperature predictions for each of the 4 GPR models for the 1122pine condition.

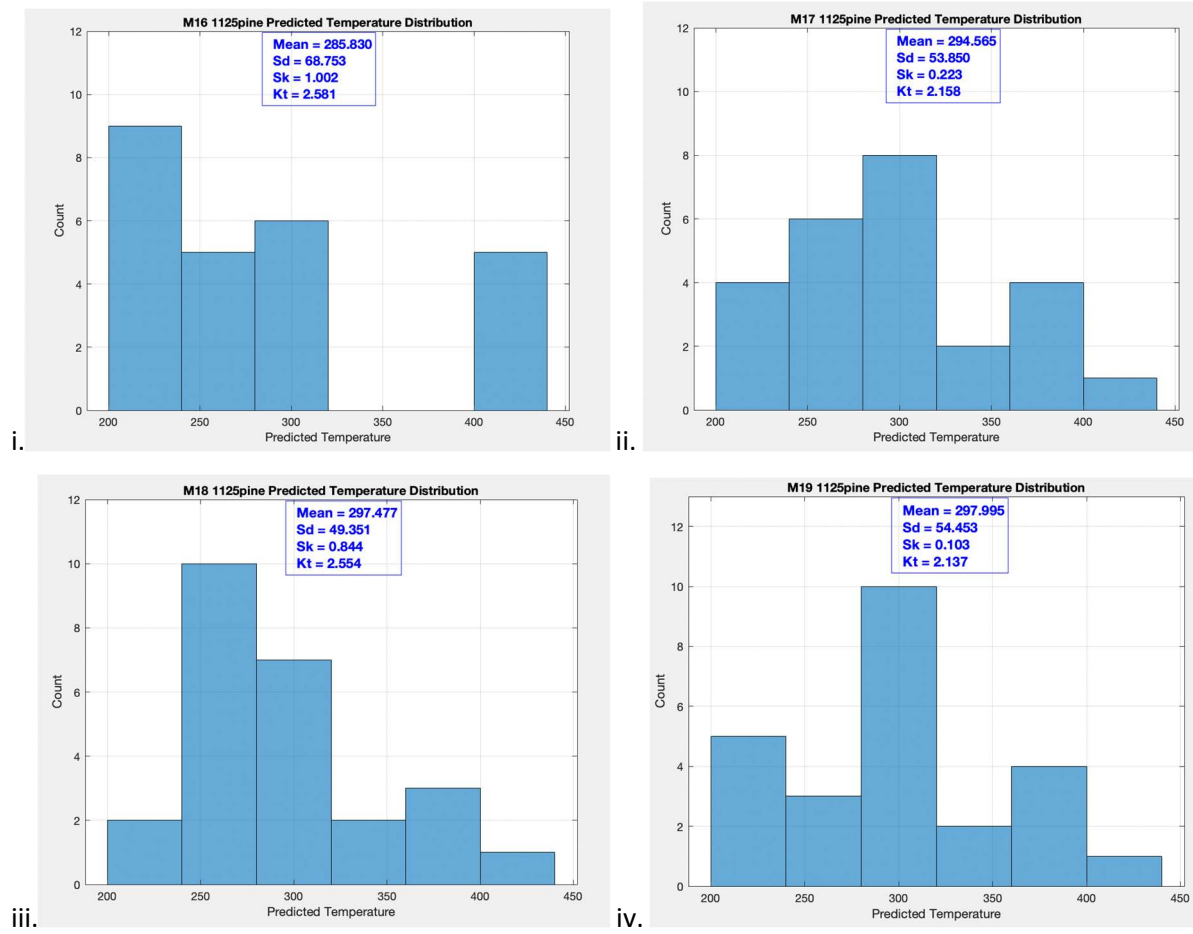
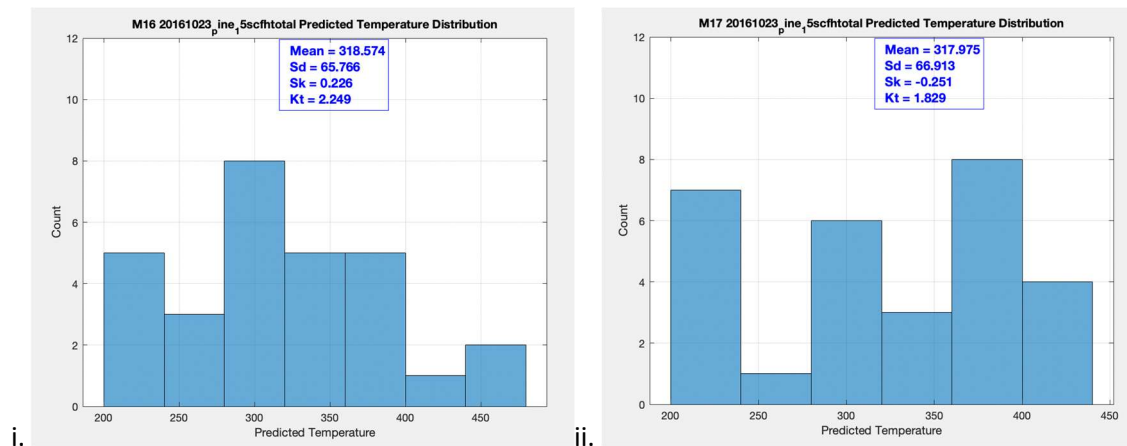


Figure 7 shows the i. Squared Exponential GPR (M16), ii. Matern 5/2 GPR (M17), iii. Exponential GPR (M18), and iv. Rational Quadratic GPR temperature prediction distribution histograms, along with the corresponding mean, Sd, Sk, and Kt for 1125pine condition.



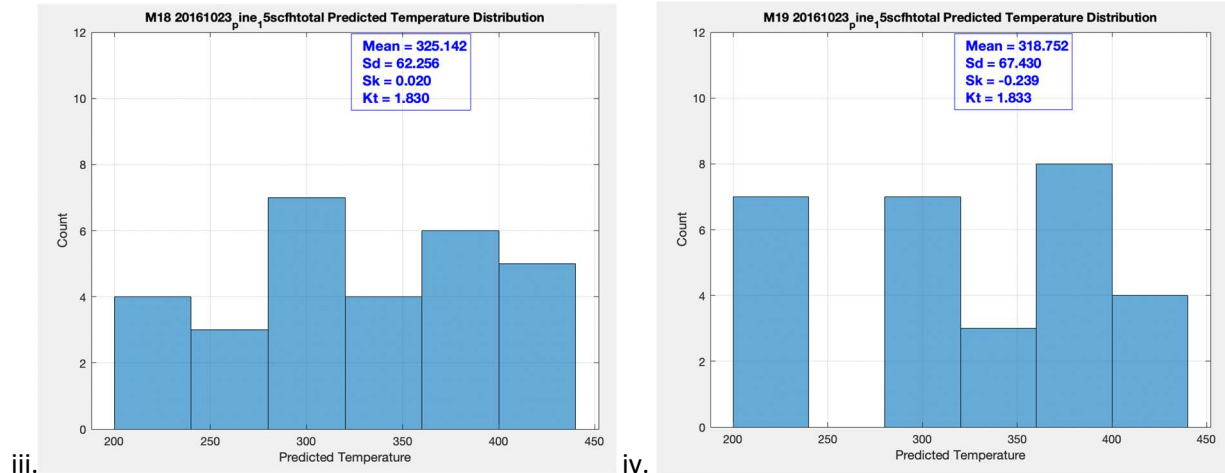


Figure 8 shows the i. Squared Exponential GPR (M16), ii. Matern 5/2 GPR (M17), iii. Exponential GPR (M18), and iv. Rational Quadratic GPR temperature prediction distribution histograms, along with the corresponding mean, Sd, Sk, and Kt for 20161023_pine_15scfhtotal condition.

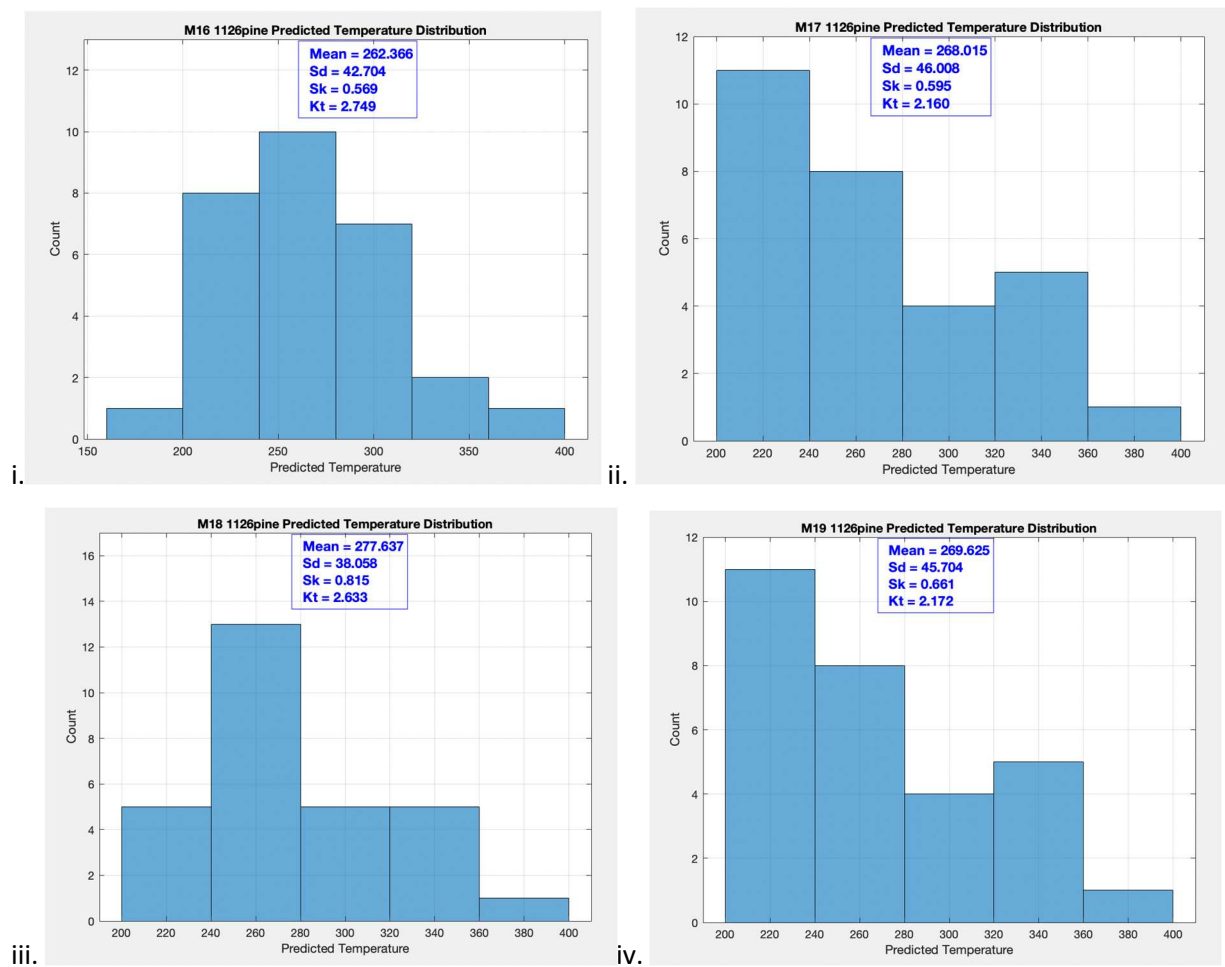


Figure 9 shows the i. Squared Exponential GPR (M16), ii. Matern 5/2 GPR (M17), iii. Exponential GPR (M18), and iv. Rational Quadratic GPR temperature prediction distribution histograms, along with the corresponding mean, Sd, Sk, and Kt for 1126pine condition.

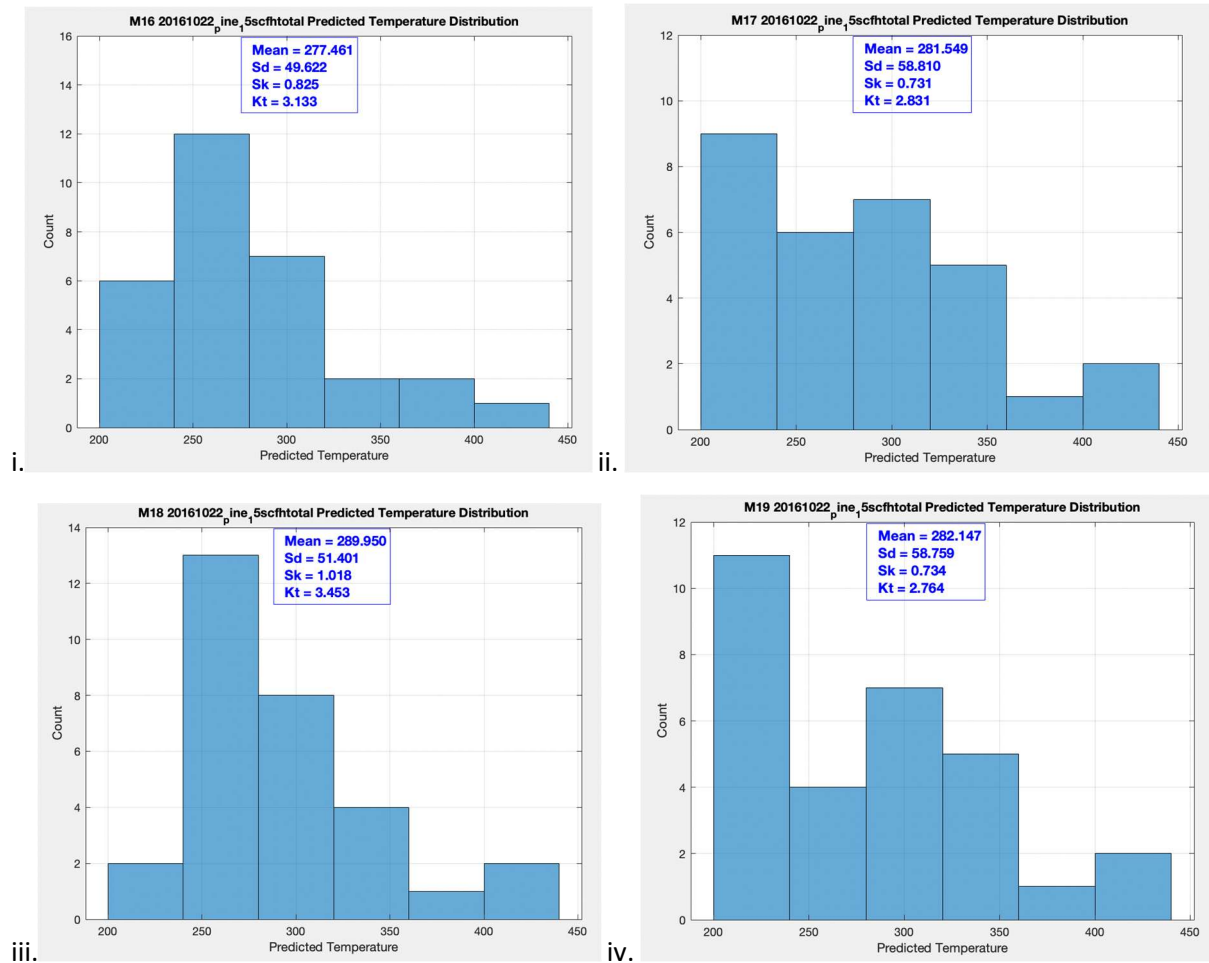


Figure 10 shows the i. Squared Exponential GPR (M16), ii. Matern 5/2 GPR (M17), iii. Exponential GPR (M18), and iv. Rational Quadratic GPR temperature prediction distribution histograms, along with the corresponding mean, Sd, Sk, and Kt for 20161022_pine_15scfhtotal condition.

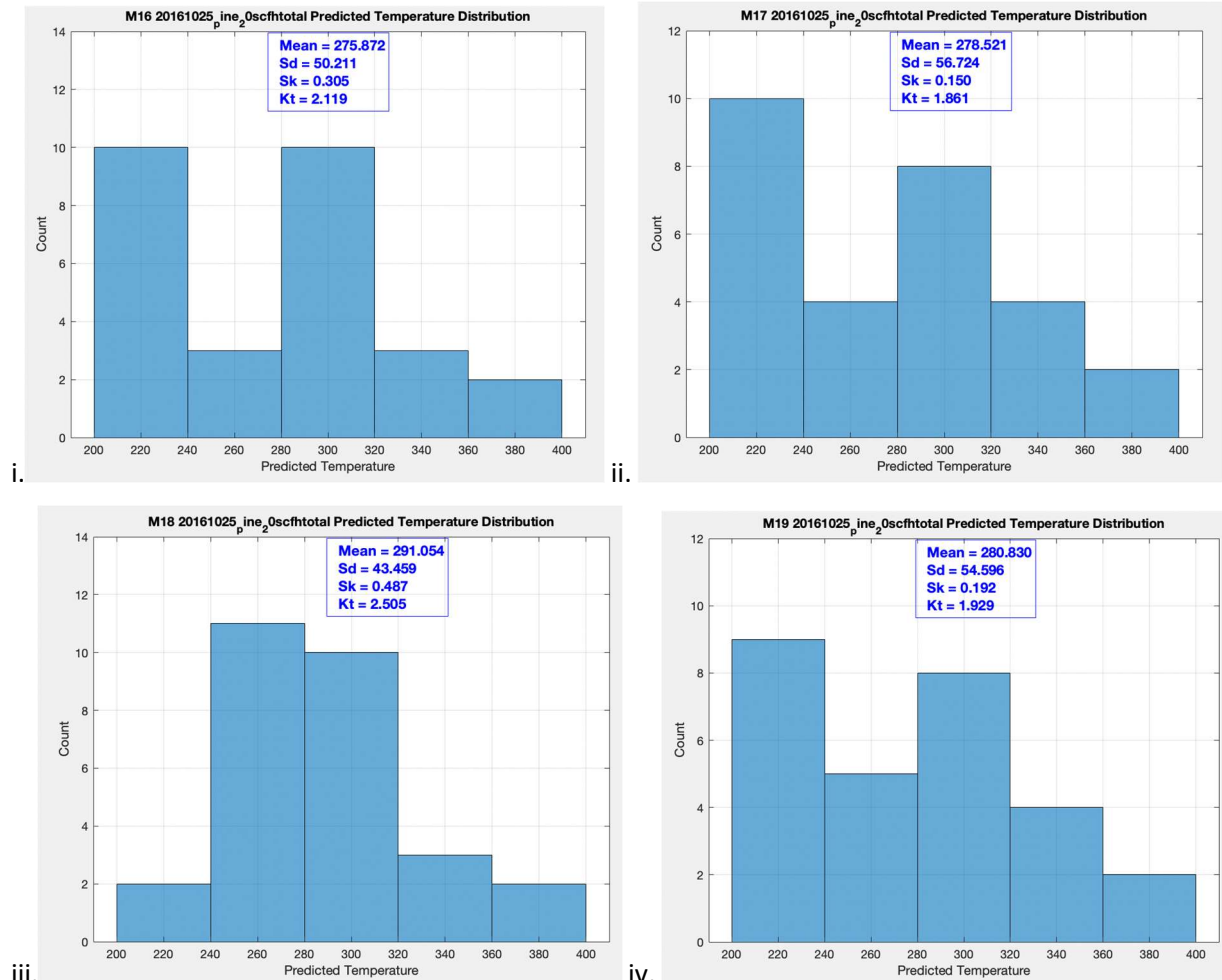
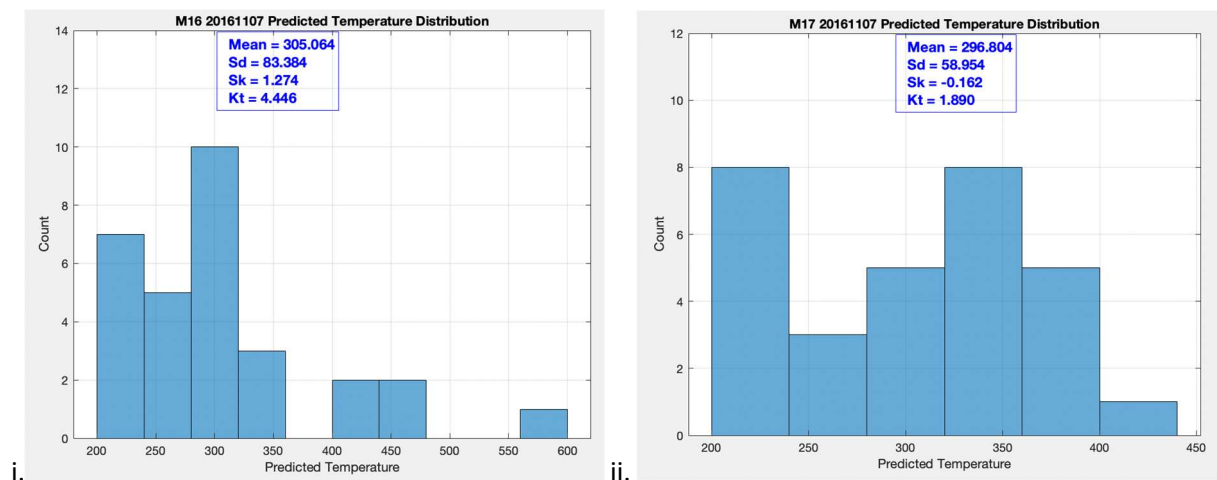


Figure 11 shows the i. Squared Exponential GPR (M16), ii. Matern 5/2 GPR (M17), iii. Exponential GPR (M18), and iv. Rational Quadratic GPR temperature prediction distribution histograms, along with the corresponding mean, Sd, Sk, and Kt for 20161025_pine_20scfhtotal condition.



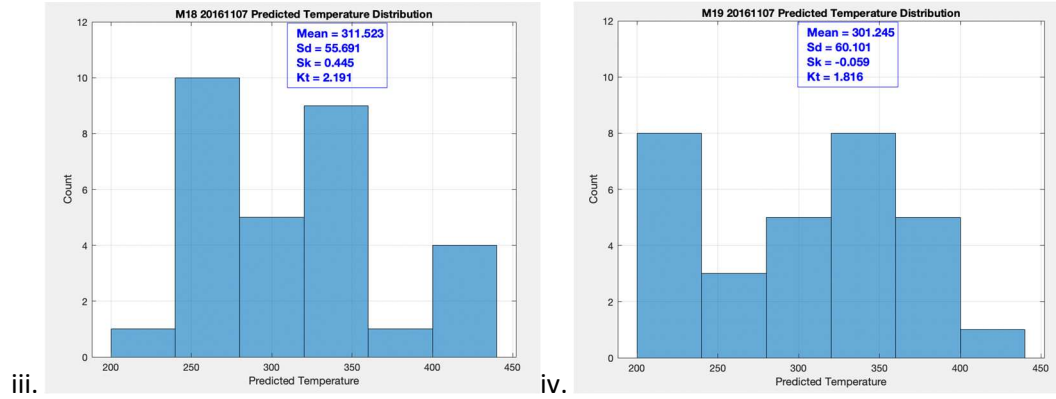


Figure 12 shows the i. Squared Exponential GPR (M16), ii. Matern 5/2 GPR (M17), iii. Exponential GPR (M18), and iv. Rational Quadratic GPR temperature prediction distribution histograms, along with the corresponding mean, Sd, Sk, and Kt for 20161107 condition.

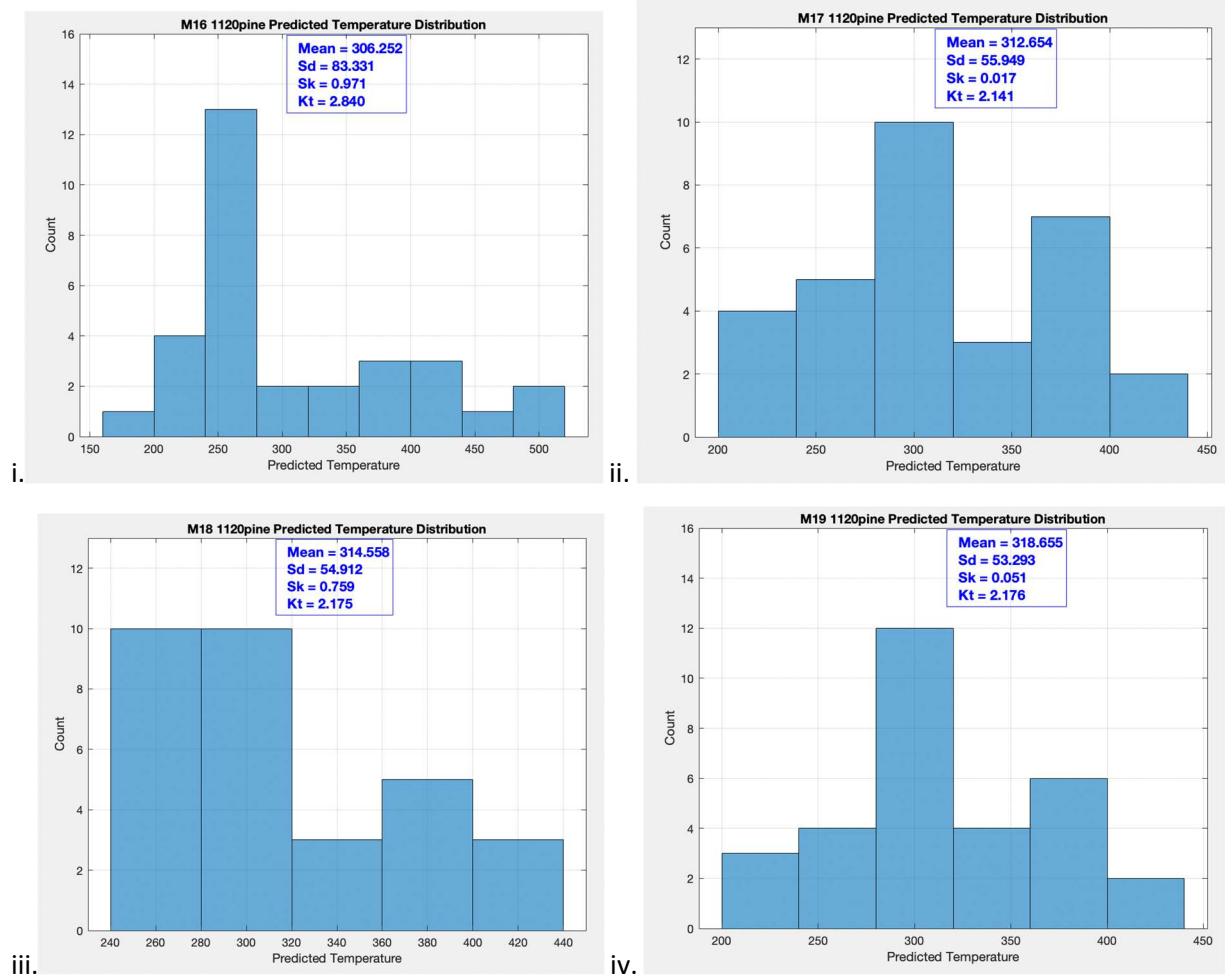


Figure 13 shows the i. Squared Exponential GPR (M16), ii. Matern 5/2 GPR (M17), iii. Exponential GPR (M18), and iv. Rational Quadratic GPR temperature prediction distribution histograms, along with the corresponding mean, Sd, Sk, and Kt for 1120pine condition.

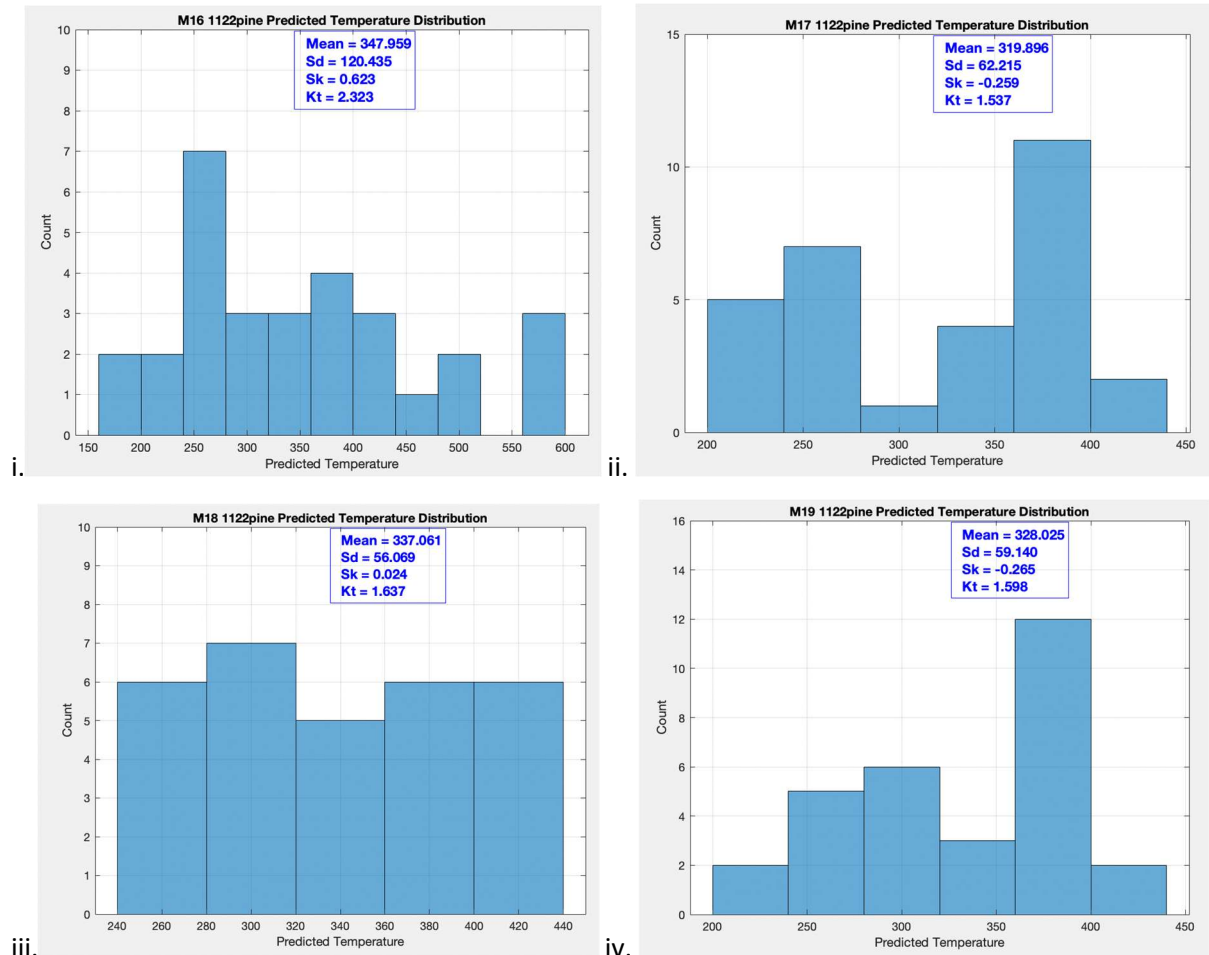


Figure 14 shows the i. Squared Exponential GPR (M16), ii. Matern 5/2 GPR (M17), iii. Exponential GPR (M18), and iv. Rational Quadratic GPR temperature prediction distribution histograms, along with the corresponding mean, Sd, Sk, and Kt for 1122pine condition.

One biomass sample (20161205_run6_proxanalysis_20161126_pine_2dot0Lperm_sample23) was removed from the 1126pine condition temperature distribution due to an erroneous spike in the TG/DTG plots likely attributable to an unintended jolt to the equipment measuring the mass.